Timing and mechanism of formation of selected talc deposits in the Ruby Range, southwestern Montana

by Dale Lewis Anderson

A thesis submitted in partial fulfillment of the requirements for the degree of Master of Science in Earth Sciences
Montana State University

Abstract:
The mechanism of formation of talc deposits in Archean dolomitic marbles of southwestern Montana is not well understood. This study examines the mineralogy, chemistry, and structure of selected talc prospects with the purpose of developing a model for talc formation in these dolomitic marbles.

Detailed field mapping and petrography yields a paragenetic sequence with three periods of mineral formation, designated , M2, and M3. M1 is characterized by amphibolite-grade assemblages in calcitic marbles. M2 resulted in dolomitization and greenschist-grade silicate assemblages overprinting M1 assemblages. M3, the last step in the paragenetic sequence, resulted in formation of talc from dolomite and all greenschist-grade silicate minerals (with the exception of chlorite) present.

Structural control of talc formation is suggested by discontinuous occurrences of talc bodies. Layer-parallel fracturing is indicated by the orientation and morphology of talc bodies, and by the lack of cross-cutting structures which can be related to talc formation.

Geochemical analyses and mass balance calculations demonstrate that talc bodies did not form by isochemical alteration of high-grade or talc-bearing marbles. Infiltration of large quantities of SiOg and Mg++ is indicated, with concomitant removal of Ca++. Infiltration is supported by the absence of isobaric univariant mineral assemblages, indicating that mineral parageneses did not buffer the talc-forming reaction.

Preservation of millimeter-to centimeter-scale relict textures suggests constant volume replacement during talc formation. Mass balance calculations show that alteration of 1 m3 0f dolomite to form talc, while conserving volume, requires addition of 1,764 kg of SiOg and 157 kg of Mg++ to the system, with concomitant removal of 1,556 kg of calcite. A minimum fluid flux of 7.05 x 1O 5 liters is indicated for each cubic meter of dolomitic marble that was altered to talc.

Field and mineralogic relationships constrain timing of talc formation. A Proterozoic, post-greenschist , pre-Paleozoic age is indicated.

Field relationships, mineral parageneses, marble and talc geochemistry, mass balance determinations, and the tectonic history of the study area are all consistent with formation of talc in a near surface hot springs environment. Maximum temperature and Pfluid indicated is 450° C and 2 kbar.

TIMING AND MECHANISM OF FORMATION OF SELECTED TALC DEPOSITS IN THE RUBY RANGE, SOUTHWESTERN MONTANA

by

Dale Lewis Anderson

A thesis submitted in partial fulfillment
of the requirements for the degree

of

Master of Science

in

Earth Sciences

MONTANA STATE UNIVERSITY
Bozeman, Montana

March, 1987

APPROVAL

of a thesis submitted by

Dale Lewis Anderson

This thesis has been read by each member of the thesis committee and has been found to be satisfactory regarding content, English usage, format, citations, bibliographic style, and consistency, and is ready for submission to the College of Graduate Studies.

3/24/87
Date

David W. Mayk
Chairperson, Graduate Committee

Approved for the Major Department

3/24/87
Date

Stephen A. Custer
Head, Major Department

Approved for the College of Graduate Studies

March 30, 1987
Date

Henry L. Parsons
Graduate Dean

STATEMENT OF PERMISSION TO USE

In presenting this thesis in partial fulfillment of the requirements for a master's degree at Montana State University, I agree that the Library shall make it available to borrowers under rules of the Library. Brief quotations from this thesis are allowable without special permission, provided that accurate acknowledgment of source is made.

Permission for extensive quotation from or reproduction of this thesis may be granted by my major professor, or in his/her absence, by the Director of Libraries when, in the opinion of either, the proposed use of the material is for scholarly purposes. Any copying or use of the material in this thesis for financial gain shall not be allowed without my written permission.

Signature Dale Anderson

Date March 24, 1987

ACKNOWLEDGEMENTS

I would like to thank David Mogk (Committee Chairman), John Childs, and David Lageson for suggestions and constructive criticism during preparation of the manuscript. Many thanks go to David Mogk and John Childs, who were particularly patient and helpful in the organization and inspection of the manuscript.

Funding for the study was provided by Cyprus Industrial Minerals Company (CIMC). CIMC also provided access to the prospects examined, and XRD analyses of selected samples. Howard Harlan of CIMC provided lodging during field work at the Metlan Annex in Dillon, Montana, as well as suggestions throughout much of the study. Andy Barth provided comments and insights during field work and early stages of the study. Michael Clark assisted with plane table mapping of the Sweetwater Mine. Rick Weeks and Robert Piniazkiewicz of Cyprus Minerals reviewed final drafts of the thesis. I thank Robert for bringing to my attention an error in the mass balance calculations, which had previously avoided detection.

Finally, I would like to thank my family, without whose support my education would not have been possible.

TABLE OF CONTENTS

TABLE OF CONTENTS--Continued

TABLE OF CONTENTS--Continued

LIST OF TABLES

LIST OF FIGURES

LIST OF FIGURES--Continued

LIST OF PLATES

ABSTRACT

The mechanism of formation of talc deposits in Archean dolomitic marbles of southwestern Montana is not well understood. This study examines the mineralogy, chemistry, and structure of selected talc prospects with the purpose of developing a model for talc formation in these dolomitic marbles.

Detailed field mapping and petrography yields a paragenetic sequence with three periods of mineral formation, designated M_1, M_2, and M_3. M_1 is characterized by amphibolite-grade assemblages in calcitic marbles. M_2 resulted in dolomitization and greenschist-grade silicate assemblages overprinting M_1 assemblages. M_3, the last step in the paragenetic sequence, resulted in formation of talc from dolomite and all greenschist-grade silicate minerals (with the exception of chlorite) present.

Structural control of talc formation is suggested by discontinuous occurrences of talc bodies. Layer-parallel fracturing is indicated by the orientation and morphology of talc bodies, and by the lack of cross-cutting structures which can be related to talc formation.

Geochemical analyses and mass balance calculations demonstrate that talc bodies did not form by isochemical alteration of high-grade or talc-bearing marbles. Infiltration of large quantities of SiO_2 and Mg^{++} is indicated, with concomitant removal of Ca^{++}. Infiltration is supported by the absence of isobaric univariant mineral assemblages, indicating that mineral parageneses did not buffer the talc-forming reaction.

Preservation of millimeter-to centimeter-scale relict textures suggests constant volume replacement during talc formation. Mass balance calculations show that alteration of 1 m^3 of dolomite to form talc, while conserving volume, requires addition of 1,764 kg of SiO_2 and 157 kg of Mg^{++} to the system, with concomitant removal of 1,556 kg of calcite. A minimum fluid flux of 7.05×10^5 liters is indicated for each cubic meter of dolomitic marble that was altered to talc.

Field and mineralogic relationships constrain timing of talc formation. A Proterozoic, post-greenschist , pre-Paleozoic age is indicated.

Field relationships, mineral parageneses, marble and talc geochemistry, mass balance determinations, and the tectonic history of the study area are all consistent with formation of talc in a near surface hot springs environment. Maximum temperature and P_{fluid} indicated is 450° C and 2 kbar.

CHAPTER 1

INTRODUCTION

Purpose and Scope

This study is part of ongoing research on the physical and chemical controls and timing of talc formation in the Ruby Range, southwestern Montana (Figure 1). The purpose of this study is to determine the mechanisms of formation of talc bodies of economic size, as well as to develop a physicochemical model for talc formation. Towards this end talc deposits have been examined in detail in the Ruby Range. Based on techniques presented below, this study will address the following points:

1) Physical characteristics of each prospect examined;
2) Talc forming reactions identified by means of petrographic analysis;
3) Geochemistry of marbles, with determination of the nature of bulk compositional changes during talc formation;
4) Mass balance calculations incorporating field and petrographic observations will demonstrate the nature of materials which may have been added to, or subtracted from, dolomitic marbles during talc formation;
5) Evidence for metasomatism, based on field relations, petrographic analysis, mass balance calculations and whole rock geochemistry;

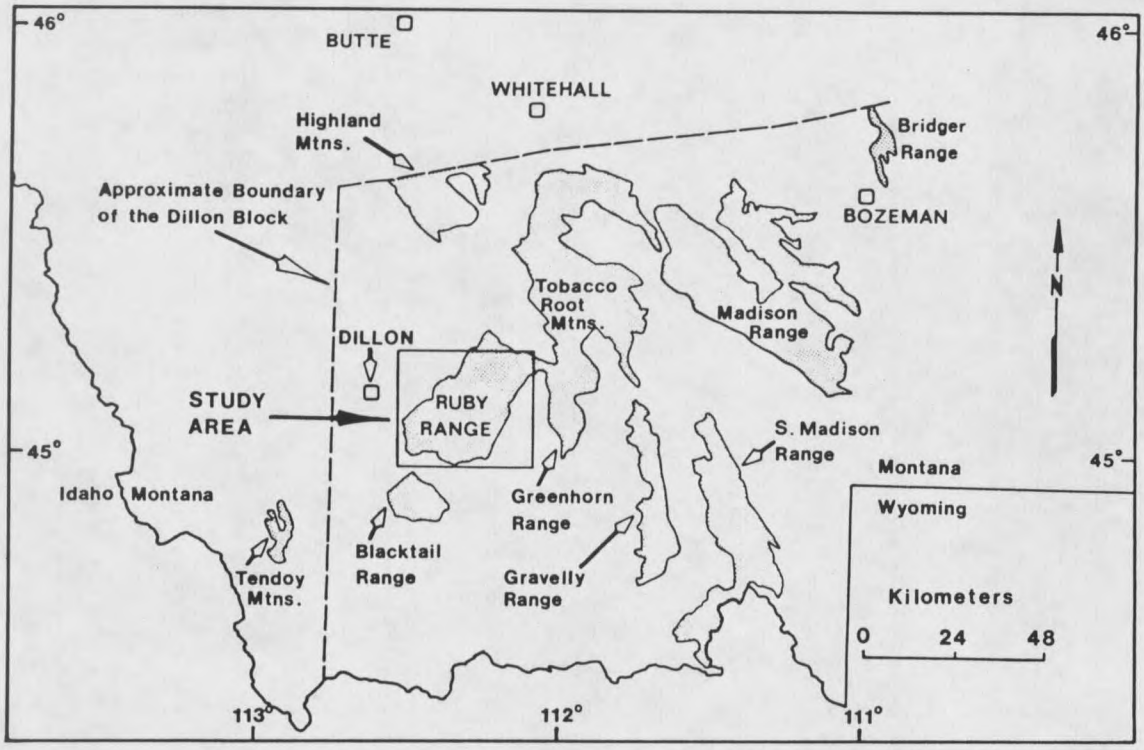

Figure 1. Regional location map showing the study area and outcrops of similar lithologies in southwestern Montana (modified from Bergantino and Clark, 1985).

6) Phase equilibria of the talc forming system and proposed temperatures of formation of talc;

7) Mechanism for formation of economic-sized talc bodies, and the inferred time of formation of such bodies.

Background

Formation of economically viable talc deposits is generally restricted to two geologic environments: 1) metamorphosed siliceous dolomitic carbonate rocks; and 2) altered ultramafic bodies. In the Ruby Range, metamorphosed dolomitic carbonate is known to be important

in talc formation; alteration of ultramafic bodies in the range has not been recognized as a mechanism for formation of minable talc bodies (Okuma, 1971; Desmarais, 1981).

Recognition of dolomitic marbles in the Ruby Range as the sole host rock for large talc deposits has resulted in several studies on the distribution and petrology of these units (Perry, 1948; Levinson, 1949; Heinrich and Rabbitt, 1960). Additional work has provided descriptions of many known talc deposits and prospects (Okuma, 1971; Garihan, 1973; Olson, 1976; Berg, 1979; Whitehead, 1979; Walton, 1981).

This study adds considerable information to this data base, including more detailed physical and petrographic descriptions of prospects studied. Also, this study results in the presentation of theories concerning talc formation which differ slightly from those developed in previous studies.

Methods

Field mapping on a scale of 1" = 5' or 1" = 10' of several talc-bearing prospects in the Ruby Range was carried out to determine mesoscopic controls on talc formation, such as compositional variations within host marbles, mineralogy, and structure. Prospects chosen for detailed examination provide three dimensional exposures of talc bodies and the relationships of talc bodies with surrounding marbles and gneisses. Also, these prospects were considered to be representative of areas with potential for talc formation of economic interest. The prospects examined during this study, shown in Figure 2, will be described in the following order: 1) Bosal Prospect; 2) Ruby View

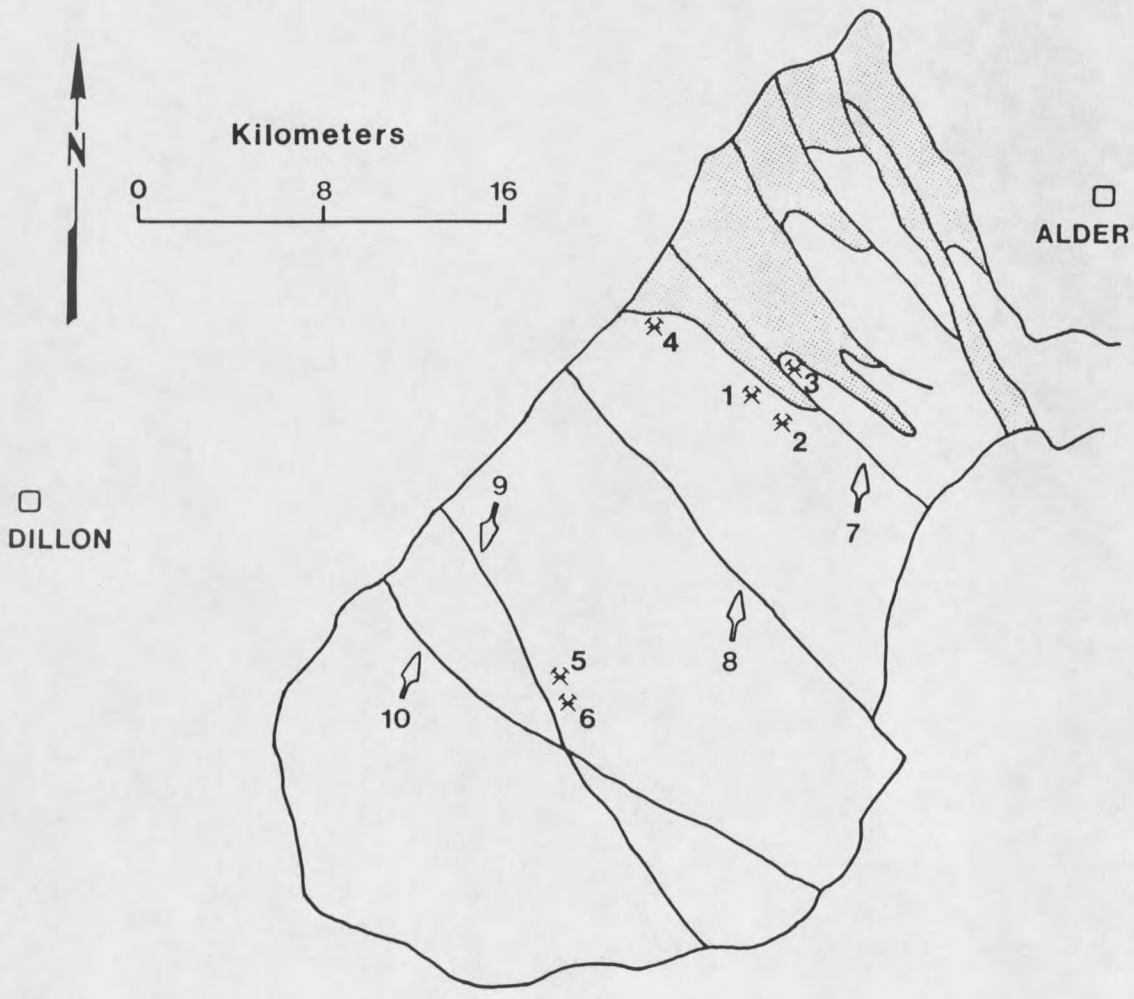

Phanerozoic Sediments

Archean Metasediments

1. Bosal Prospect
2. Ruby View Prospect
3. T.P. Prospect
4. Spring Creek Prospect
5. Pope Prospect
6. Sweetwater Mine
7. Cottonwood Creek Fault
8. Stone Creek Fault
9. Carter Creek Fault
10. Sweetwater Fault

Figure 2. Location map showing the Ruby Range, with locations of prospects examined, and major northwest trending faults (modified from Schmidt and Garihan, 1986).

Prospect; 3) T.P. Prospect; 4) Spring Creek Prospect; 5) Pope Prospect; and 6) the Sweetwater Mine. All of the prospects examined are controlled by Cyprus Industrial Minerals Company (CIMC).

Samples collected during mapping were analyzed using standard petrographic techniques, as well as cathodoluminesence (CL) and ultraviolet (UV) microscopy, with two main goals: 1) determination of the talc-forming reactions; and 2) understanding the nature of talc-forming reactions within the context of the paragenetic sequence and thermal history of marbles being examined.

Samples were selected for whole rock geochemical analysis to determine chemical differences between talcose and non-talcose marbles. This information is necessary to evaluate the possible metasomatic processes which were active during talc formation.

Geologic Setting

In southwestern Montana, economically viable talc occurrences are restricted to Archean marbles exposed in late-Cretaceous-to Paleocene-aged block uplifts which have been modified by subsequent Basin and Range extension. Such lithologies occur in the Ruby, Tobacco Root, Gravelly, and Tendoy Ranges, among others (Berg, 1979) (Figure 1). All talc prospects examined during this study are located in marbles which have been correlated with the Cherry Creek Group (Heinrich and Rabbitt, 1960; Okuma, 1971; Garihan, 1973), as defined by Peale (1896), in the Gravelly Range, south of Ennis, Montana. This correlation has not been verified by geochronologic or geochemical data.

Previous investigators in the Ruby Range generally agree that the area underwent amphibolite-to granulite-grade, dynamothermal metamorphism (M_1), dated at approximately 2750 Ma. (Gilletti, 1966; Okuma, 1971; Garihan, 1973; James and Hedge, 1980). M_1 metamorphism produced the dominant foliation within the central and southern Ruby Range, which strikes northeast and dips to the northwest (Karasevich and others, 1981). Macroscopic folds associated with M_1 are isoclinal to tight, and axial surfaces strike northeast, and dip to the northwest. This style of folding is correlative with F_1 and F_2 folds of Okuma (1971) in the southern portion of the range, and F_1 and F2 folds of Garihan (1973) in the central portion of the range. Deformation of isolated quartz pods and development of boudinage in gneiss and schist lenses within marble described herein is interpreted as having formed under these conditions. Timing of Okuma's F_3 event with respect to metamorphic conditions is unclear, but it is thought to have occurred under amphibolite-grade conditions due to a poorly developed axial planar cleavage (?) defined by alignment of hornblende and biotite in F_3 folds (Okuma, 1971).

A Proterozoic retrograde regional thermal event (M_2) resulted in overprinting of the amphibolite-grade assemblages by greenschist facies assemblages. No penetrative deformational features are associated with this thermal event. K-Ar dates place the timing of M_2 at about 1600 Ma. (Giletti, 1966; Okuma, 1971; Garihan, 1973; Dahl, 1979; Desmarais, 1981).

Talc formation (M_3) occurred very late-to post-retrograde greenschist mineralization (M_2). It is important to point out that the

M_3 event may not represent a separate orogenic cycle; rather it may represent the final stage of M_2 recrystallization.

The major faults in the Ruby Range strike northwest (Figure 2), and have undergone recurrent movement since Proterozoic time (Schmidt and Garihan, 1983, 1986). Previous workers have suggested that talc formation is the result of fluid movement along these structures during the Proterozoic greenschist thermal event (Okuma, 1971; Garihan, 1973; Olson, 1976; Berg, 1979).

Contemporaneous with, and possibly prior to incipient rifting of the Belt Basin (1700 - 1500 Ma.), several generations of northwest trending mafic dikes intruded the area, probably along pre-existing fracture zones (Wooden and others, 1978). It has been postulated that these dikes may have been the source of heat and fluids for talc formation (Wooden and others, 1978). However, no apparent spatial relationship between mafic dikes and talc-bearing marble was documented during this study.

The Ruby Range and surrounding area (termed the Dillon Block by Harrison and others (1974))(Figure 1), has been interpreted as a positive tectonic feature during middle-to late-Proterozoic time, acting as the source area for clasts of Archean marble, gneiss and amphibolite in the LaHood Formation, which was deposited on the southern margin of the Belt Basin (McMannis, 1963; Boyce, 1975). Deposition of the LaHood Formation has been interpreted as marking incipient rifting of the Belt Basin (McMannis, 1963).

The northern-most portion of the Ruby Range is underlain by Phanerozoic sediments which have been subjected to Laramide style

deformation (Tysdal, 1976; Schimdt and Garihan, 1983). Most recently Basin and Range style extension has overprinted Laramide style deformation.

CHAPTER 2

FIELD RELATIONSHIPS AND PETROGRAPHY

Bosal Prospect

Introduction

The Bosal Prospect, controlled by CIMC, (Figure 2, SE 1/4 Sec.11 T7S R6W) is an isolated talc occurrence within a continuous marble band up to 20 meters thick. This marble band probably forms one limb of a tight to isoclinal fold, whose axial surface strikes northeast and dips steeply northwest. Compositional layering is defined in high-grade marbles by bands rich in Mg silicates, striking N 50-70° E and dipping 50-60° northwest. Centimeter-scale open folds and warps in layering are common. The geology of the prospect is shown in Plate 1.

High-Grade Marble

High-grade marbles (includes those marbles with mineral assemblages indicative of high metamorphic grade) tend to be more calcitic than talc-bearing marbles, and contain the assemblage calcite-olivine-phlogopite +/- dolomite.

In thin section, carbonate grains display irregular to rounded boundaries and patchy extinction, undulose extinction is rare. Twinning in carbonate grains is present but not abundant. A complex recrystallization history is indicated by calcite grains which exhibit

homogeneous rims of calcite surrounding well developed exsolution (dolomite from calcite) lamellae.

On a microscopic scale retrograde serpentine occurs dominantly as a replacement of olivine, often with small growths of serpentine into surrounding dolomite grains. Small rounded calcite grains are common in serpentine that has replaced olivine grains, possibly a by-product of the recrystallization of olivine and dolomite to form serpentine by the reaction:

1 Olivine + 1 Dolomite + 1 Quartz + 8 H_2O = 1 Serpentine + 1 $CaCO_3$ + 1 CO_2 + 6 H_2O (Tables 1 and 2).

Quartz present in high-grade marbles occurs as deformed lenses and as rare isolated, secondary grains within marble.

Talc-Bearing Marble

Talc-bearing marbles contain the assemblage dolomite-calcite-talc-chlorite. Serpentine, tremolite and relict phlogopite are also present but are not in equilibrium. Graphite, pyrite, manganese oxide, and rare quartz are present as accessory minerals. Textures indicating the presence of a stable mineral assemblage are not present. Figure 3 shows the paragenetic sequence determined for the Bosal Prospect.

A complex recrystallization history is indicated by carbonate textures. These textures also indicate that the main period of dolomite formation post-dates high-grade metamorphism, in that all exsolution textures observed involved dolomite exsolving from calcite (Figure 4).

The dominant carbonate in talc-bearing marble is dolomite, which varies in color from light-orange to brown to white. Grains are subhedral to anhedral and range in size from 1 millimeter (mm) to 1 centimeter (cm), averaging 1 mm to 2 mm. Average grain size varies between layers.

Table 1. Summary of replacement reactions and diablastic intergrowths observed during petrographic analysis, and the prospects in which they occur. Abbreviations used here are used in all following diagrams. R.V. (Ruby View), S. Creek (Spring Creek), Do (dolomite), Tc (talc), S (serpentine, Ch (chlorite), Tr (tremolite), Feld (feldspar), Qtz (quartz), Ph (phlogopite), Cc (calcite), Ol (olivine).

Prospect:	Bosal	R. V.	T.P.	S. Creek	Pope	Sweetwater
Observed Replacement						
1) Do -- Tc	X	X	X	X		
2) S -- Tc	X	X	X	X	X	
3) Ph -- Tc	X	X	X	X		
4) Tr -- Tc	X	X		X	X	
5) Qtz -- Tc				X		X
6) M -- Tc						X
7) Ph -- Ch	X			X		
8) Qtz -- S		X				
9) Ol -- S	X		X		X	
10) Tr -- S					X	
11) Feld -- Ch						X
Diablastic Intergrowths						
1) Ch -- Tc	X	X	X	X	X	
2) Do -- Ch		X		X	X	
3) Do -- S	X					
4) Ch -- S		X	X	X		
5) Cc -- Tc					X	

Table 2. Balanced reactions corresponding to replacement reactions presented in Table 1.

---

1) Do--Tc: $3\ CaMg(CO_3)_2 + 4\ SiO_2 + 1\ H_2O = 1\ Mg_3Si_4O_{10}(OH)_2 + 3\ CaCO_3 + 3\ CO_2$

2) S--Tc: $1\ Mg_3Si_2O_5(OH)_4 + 2\ SiO_2 = 1\ Mg_3Si_4O_{10}(OH)_2 + 1\ H_2O$

3) Ph--Tc: $4\ KMg_3(AlSi_3O_{10})(OH)_2 + 4\ SiO_2 + 4\ H_2O = 4\ Mg_3Si_4O_{10}(OH)_2 + 4\ KOH + 2\ H_2O$

4) Tr--Tc: $1\ Ca_2Mg_5Si_8O_{22}(OH)_2 = 1\ Mg_3Si_4O_{10}(OH)_2 + 4\ SiO_2 + 2\ CaO + 2\ MgO$

5) Qtz--Tc: $4\ SiO_2 + 3\ Mg(OH)_2 = 1\ Mg_3Si_4O_{10}(OH)_2 + 2\ H_2O$

6) M--Tc: $3\ MgCO_3 + 4\ SiO_2 + 1\ H_2O = 1\ Mg_3Si_4O_{10}(OH)_2 + 3\ CO_2$

7) Ph--Ch: $10\ K\ Mg_3(AlSi_3O_{10})(OH)_2 + 1\ Al_2O_3 + 29\ H_2O = 6\ Mg_5Si_3Al_2O_{10}(OH)_8 + 10\ KOH + 12\ SiO_2$

8) Qtz--S: $2\ SiO_2 + 3\ Mg(OH)_2 = 1\ Mg_3Si_2O_5(OH)_4 + 1\ H_2O$

9) Ol--S: $1\ Mg_2SiO_4 + 1\ CaMg(CO_3)_2 + 1\ SiO_2 + 8\ H_2O = 1\ Mg_3Si_2O_5(OH)_4 + 1\ CaCO_3 + 1\ CO_2 + 6\ H_2O$

10) Tr--S: $3\ Ca_2Mg_5Si_8O_{22}(OH)_2 + 15\ H_2O = 5\ Mg_3Si_2O_5(OH)_4 + 6\ CaO + 14\ SiO_2 + 8\ H_2O$

11) Feld--Ch: $2\ KAlSi_3O_8 + 5\ Mg(OH)_2 = 1\ Mg_5Si_3Al_2O_{10}(OH)_8 + 2\ KOH + 3\ SiO_2$

Talc occurs in several forms including: 1) a large layer-parallel body which is locally discordant; 2) centimeter-scale irregularly shaped talc pods which do not appear to be controlled by layering or fracturing; 3) scattered veinlets parallel to layering; and 4) disseminated talc grains which in many cases exhibit pseudomorphs after dolomite and tremolite.

The main talc body is a layer-parallel unit 2.5 to 3.5 meters (m) thick. Incomplete alteration of marble to talc within the body is indicated by inclusions of relict marble blocks.

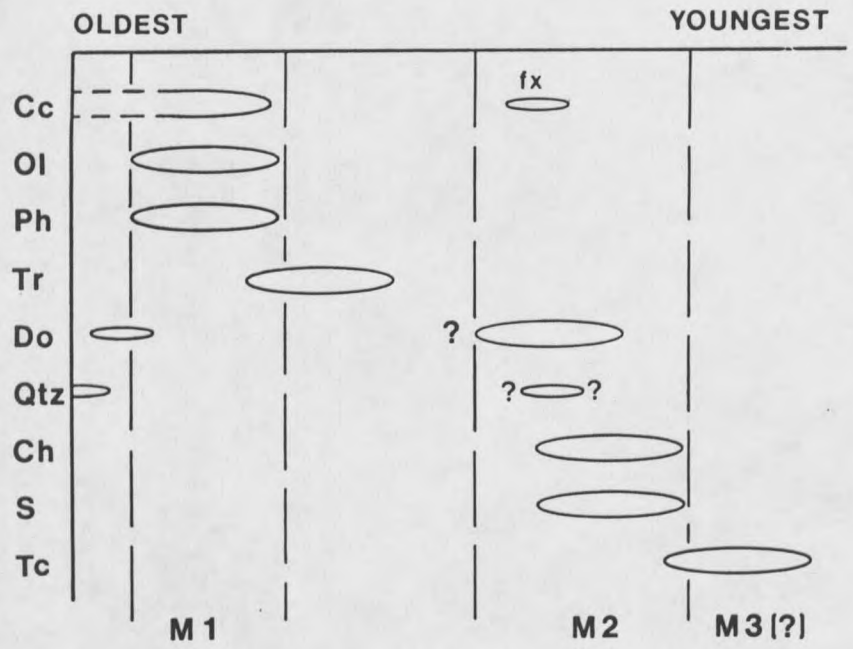

Figure 3. Diagram showing the paragenetic sequence determined for the Bosal Prospect. Fx (fracture filling).

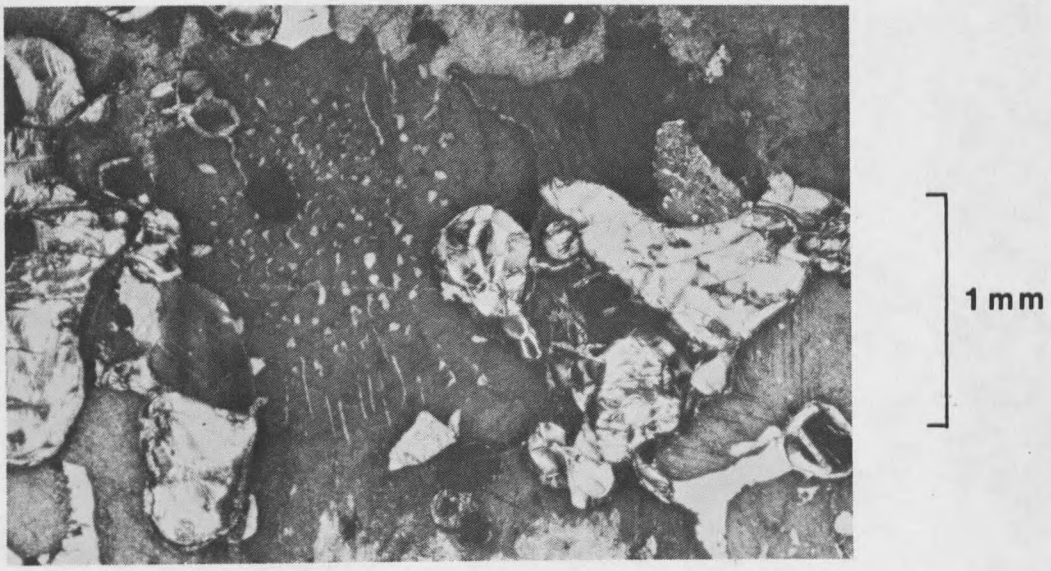

Figure 4. Photomicrograph showing exsolution lamellae in carbonates (dolomite exsolving from calcite).

In thin section, talc is seen as cryptocrystalline masses with inclusions of chlorite, serpentine, phlogopite, and rare apatite. Accessory pyrite with limonite halos is also common within talc. Inclusions frequently occur as clots up to 5 mm in diameter composed of a mosaic of the above listed minerals (minus pyrite and apatite). Serpentine and phlogopite have recrystallized to form talc; chlorite forms diablastic intergrowths with talc.

A discontinuous 5 cm to 10 cm thick dark gray alteration zone composed of talc, minor graphite, and intensely argillized amphibolite is found at the contact between talc-bearing marble and the overlying Dillon Gneiss. Argillization does not extend into gneiss or marble for more than ten to twenty centimeters.

Dillon Gneiss

Dillon Gneiss conformably underlies the Bosal marble, and contains the amphibolite-grade assemblage plagioclase(An_{14-54})-amphibole(cummingtonite)-biotite, with rare quartz. This unit has undergone intense chloritic alteration, with the degree of alteration lessening with distance from the marble-gneiss contact. A greenschist facies assemblage of chlorite-sericite-serpentine overprints the above mentioned amphibolite-grade assemblage. Also present are minor talc stringers, rare quartz and fine-grained carbonate. Retrograde chlorite (with minor serpentine) fills fractures in gneiss both parallel to, and cross-cutting foliation. In rare cases, serpentine which is present within chlorite-filled fractures exhibits a well developed halo of chlorite.

Carbonate within altered gneiss exhibits textures suggesting influx of carbonate-bearing fluids. Carbonate is more wide-spread than is chlorite, being present throughout the rock, while chlorite is largely restricted to fractures. The phase which carbonate is replacing can not be positively identified, but is thought to be plagioclase.

Structure

Faults within the prospect area are dominantly northwest-striking, and dip to the northeast. Latest movement on faults is reverse-oblique slip, and post-dates talc mineralization. Total offset is generally less than 30 cm.

Joints within the prospect strike dominantly to the northwest, and dip to the southwest. Joint and layering surfaces are typically coated by thin selvages of talc, chlorite, or iron oxide. Deformation related to formation of talc is not evident. Structures responsible for localization of talc formation are no longer discernible.

Summary

High-grade marbles with the assemblage calcite-olivine-phlogopite +/- dolomite are overprinted by greenschist-grade assemblages, and by formation of dolomite. Talc occurs as an alteration product of dolomite and serpentine, indicating that talc formation was either the last stage of greenschist recrystallization, or a separate post-greenschist event. Mineral relationships do not permit a distinction to be made between these two possibilities.

Deformation resulting from talc formation, in the form of faulting or distortion of layering, is not noted on an outcrop scale. Also, structures which may have provided large volume conduits for fluid movement are no longer visible. However, it is obvious that talc-forming fluids migrated at least in part along joint and layering surfaces, and along lithologic contacts, as evidenced by thin selvages of talc along these surfaces. Marble and gneiss were both affected by hydrothermal alteration, with evidence present for carbonate influx into gneisses.

Ruby View Prospect

Introduction

The Ruby View Prospect, controlled by CIMC, (Figure 2, NW 1/4 Sec. 13, T7S R6W) is located approximately at the apex of a small flexure in the same marble band currently being mined by Pfizer Corp., approximately 2 km to the northwest (NW 1/4 Sec.14, T7S R6W). Compositional layering, locally defined by talc stringers standing in positive relief on weathered surfaces, strikes N 50-60° W, and dips 30-50° northeast. The geology of the Ruby View Prospect is shown in Plate 2.

High-Grade Marble

Marbles with high-grade mineral assemblages tend to be more calcitic than are talc-bearing marbles, an observation which is true in all prospects examined during this study. These rocks contain an assemblage of calcite-diopside-olivine +/- phlogopite. Scattered layers are garnetiferous.

Serpentine-Bearing Marble

Calcite-serpentine marble +/- quartz is present 8 m southeast and 45 m northwest of the Ruby View Prospect. Approximately 350 m west of the prospect calicite-serpentine +/- quartz marble changes abruptly to the calcite-diopside-olivine (+/- garnet) marble mentioned above. This transition marks the western boundary of greenschist-grade mineralization in the immediate area.

Talc-Bearing Marble

Talc-bearing marbles in the Ruby View Prospect are medium (2-4 mm)-to coarse (>4 mm)-grained, dolomitic, and contain the greenschist-grade assemblage dolomite-calcite-talc-chlorite. Evidence for equilibrium is lacking within the greenschist-grade assemblage. Other phases present (also not in equilibrium) include serpentine, and relict tremolite and phlogopite. A single occurrence of relict calcite-diopside (minus olivine) was noted within talc-bearing marble, found within 1 m of a dolomite-talc assemblage. Graphite and pyrite are present as accessory minerals. Quartz is notably absent in hand sample or thin section. The paragenetic sequence determined for the Ruby View Prospect is presented in Figure 5.

Evidence for multiple generations of dolomite is present, but rare. Where present, it is manifested as undulose and patchy extinction in dolomite grains, and as occasional recrystallized rims on earlier-formed grains. Coarse dolomite crystals up to 1 cm in size occur as vug-fillings in several places within the prospect.

Calcite, subordinate in quantity to dolomite, occurs as matrix-forming grains, and tends to be finer grained than dolomite. Calcite

exhibits rare textures similar to those seen in dolomite, indicating the presence of multiple generations of calcite. Calcite formed by the alteration of dolomite to talc (Tables 1 and 2) has not been identified using normal petrographic methods, or by UV and CL microscopy.

Talc in the Ruby View Prospect occurs in several forms including: 1) a massive body dominantly parallel to layering; 2) concordant elliptical lenses; 3) irregular millimeter-to centimeter-scale botryoidal blebs which occur as open space fillings within vugs lined by coarsely crystalline dolomite; 4) replacement of coarse poikiloblastic dolomite grains; 5) disseminated grains (often micaceous); 6) small lenses in hinge zones of meter-scale open folds in marble; and 7) as discontinuous coatings on poorly exposed layering planes.

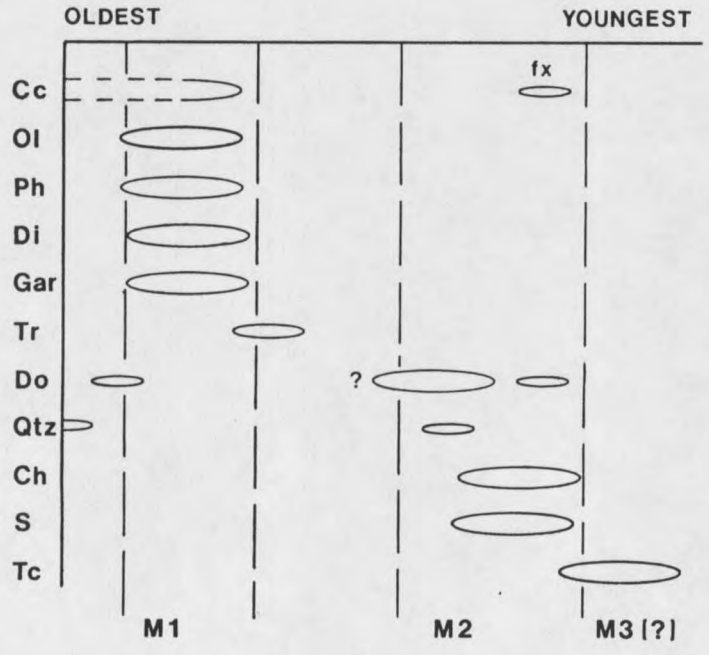

Figure 5. Diagram showing the paragenetic sequence developed for the Ruby View Prospect. Gar (garnet), Di (diopside).

The main talc body is oriented roughly parallel to layering within surrounding marble, and is up to 2.5 m in true thickness. Talc varies from light-green, high-purity material, to gray-brown talc with abundant impurities. Impurities are mainly dolomite, graphite and tremolite. Pseudomorphs of talc after dolomite are common, talc pseudomorphs after tremolite are present but not abundant.

Examination of the talc body where exposed along strike indicates a maximum lateral extent of 9 m to 12 m. Termination of the body is apparently due to a gradual pinch-out, as opposed to fault controlled termination.

In addition to the main talc body there are several elliptical talc lenses present, generally concordant to layering, with flat to convex borders. These bodies range from 0.3 m to 1.5 m in length, and 15 cm to 60 cm in thickness. Halos of partial talc replacement up to 15 cm in width surround many of these talc lenses. However, this feature is inconspicuous in outcrop because the original texture and color of the marble are well preserved.

The hinge zone of a meter-scale, gentle to open fold (F_3?) in the northwestern portion of the prospect contains a lens of talc 4 cm to 8 cm thick which pinches out along fold flanks. The axial plane of this fold strikes N 30° E and dips 80° SE, with a fold axis which trends N 26° E and plunges 47° NE. This talc lens exhibits a geometry analogous to saddle reefs in precious metal deposits. Talc formation of this type is interpreted as being the result of small-scale variations in pressure during talc formation, with talc forming in areas of relatively low pressure.

On a microscopic scale talc occurs as an alteration product of dolomite, phlogopite, and serpentine, and is associated with chlorite (Tables 1 and 2). Pseudomorphs of talc after serpentine and dolomite are common.

Summary

Dolomite and calcite exhibit a complex history of recrystallization, with multiple generations of both carbonates present. Talc formation can not be genetically related to any of the carbonate generations observed.

The main talc body, layer-parallel in form, pinches out along strike. Structural controls responsible for talc formation in this restricted zone of talc growth are not apparent.

T.P. Prospect

Introduction

The T.P. Prospect is controlled by CIMC. The main T.P. marble (Figure 2, NE 1/4 Sec. 13, T7S R6W), as well as a small marble lens to the northwest (herein informally designated as the upper T.P. marble) are concordant marble bands within Dillon Gneiss (Garihan, 1973). Compositional layering, defined by Mg silicate-rich bands strikes N 50-80° E, dipping 45-60° northwest. Foliation in adjacent gneisses strikes N 78° E, dipping 46° northwest. Refer to Plate 3 for a geologic map of the prospect area.

High-Grade Marble

The main T.P. marble away from the talc zone, and the upper T.P. marble are quite similar to each other, and notably different from marble in the immediate proximity of the talc body. Outlying marbles are fine-to coarse-grained (2mm - 10 mm), and contain the assemblage calcite-dolomite-olivine. Quartz is also present as disharmonically folded stringers and as discrete secondary grains within vugs. Retrograde minerals consist solely of serpentine, which forms pseudomorphs after olivine. Accessory graphite is present, but is of indeterminant age. High-grade marbles are commonly vuggy, with abundant red to yellow iron oxide coatings within vugs. Cross-cutting metallic to submetallic hematite veinlets are common, and locally abundant.

On a microscopic scale, high-grade calcitic marbles generally exhibit multiple generations of carbonate growth manifested as: 1) zones of patchy extinction; 2) thin recrystallized rims around earlier formed grains; and 3) carbonate veinlets which cross-cut serpentine grains. Calcite commonly exhibits well developed exsolution lamellae of dolomite. Grains containing exsolution lamellae commonly exhibit homogeneous recrystallized rims of calcite.

Also in thin section, quartz, with rhombohedral dolomite inclusions, fills vugs with either rhombohedral or irregular outlines. Using UV microscopy, quartz is seen to occur: 1) as thin layers along growth zones in rhombohedral dolomite; 2) as partial to complete infillings of vugs; and 3) as late-stage fracture fillings. In plane

light quartz layers along growth zones and late-stage fracture fillings are masked by ubiquitous iron oxide staining.

Talc-Bearing Marble

Talc-bearing marble within the prospect is medium-to coarse-grained, with an assemblage of dolomite-calcite-talc-chlorite. Evidence for equilibrium is lacking. Also present, but not in equilibrium are phlogopite, serpentine, and graphite. Variations in composition between marble layers apparently controls the abundance of disseminated talc, phlogopite, serpentine, and chlorite present in any given marble layer. The paragenetic sequence for the T.P. Prospect is presented in Figure 6.

In thin section, dolomite exhibits several distinct morphologies: 1) discrete grains; 2) rims on earlier formed calcite grains; 3) thin replacement zones along cleavage traces in calcite; 4) fracture-fillings which crosscut calcite grains; and 5) concentrations along grain boundaries of calcite. Patchy and undulose extinction in dolomite is present but not common. Calcite also exhibits evidence for the presence of multiple generations manifested by patchy extinction of calcite grains.

Talc within the T.P. Prospect occurs in several forms including: 1) a large, layer-parallel body which is slightly discordant; 2) as thin coatings along joints and layering surfaces; and 3) disseminated grains within marble (often forming pseudomorphs after serpentine (Figure 7).

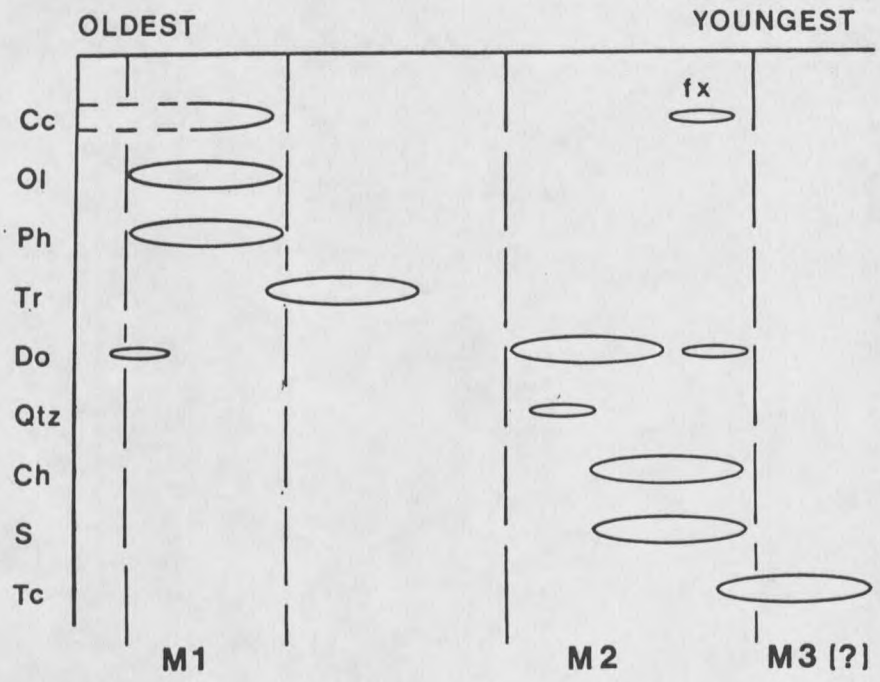

Figure 6. Diagram showing the paragenetic sequence for the T.P. Prospect.

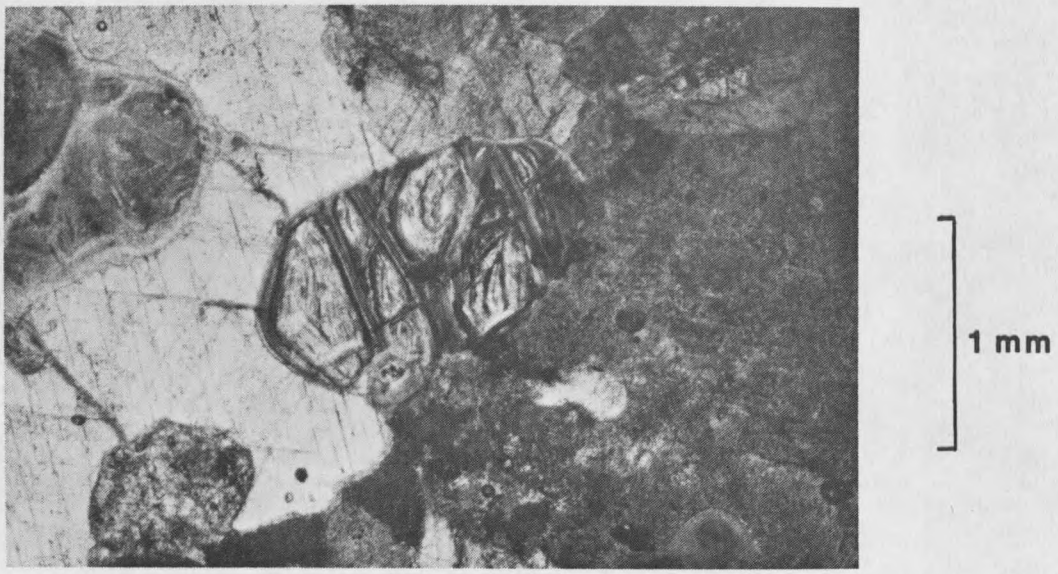

Figure 7. Photomicrograph showing talc pseudomorphs after serpentine.

The main T.P. talc body is exposed within the prospect for approximately 30 meters along strike. Layering within talc mimics original marble layering, and is roughly parallel to compositional layering noted in marble overlying the talc body. The contact of talc with overlying marble is nearly concordant, diverging from layering by 5-10° (Plate 3). A 2 cm to 6 cm thick argillized and graphitic zone is common at the contact of the talc body with overlying marble. The base of the talc body, as well as the eastern termination of the body, are not well enough exposed to determine relationships with the surrounding marble; this also precludes determination of true thickness of the talc body. A northeast-trending shear zone which dips steeply southeast marks the western termination of the talc body. Amount of offset on this shear can not be determined due to lack of exposure.

Talc within the main body is dark-green in color and contains abundant talc pseudomorphs after serpentine. Chalcopyrite (?) makes up 0.5 % to 1% of the talc body and is locally altered to hematite. Copper and/or iron staining is common along fractures in talc. Incomplete alteration of marble to talc is indicated by rare relict marble blocks within the main talc body.

On a microscopic scale talc occurs as an alteration product of dolomite, serpentine, and phlogopite. In dolomitic marbles with pseudomorphs of talc after serpentine, talc commonly forms halos which extend into dolomite grains adjacent to talc grains.

Dillon Gneiss

Dillon gneiss surrounding the lower T.P. marble band is unaltered on outcrop or hand sample scale, with the exception of local isolated

blooms of chlorite. Gneiss underlying the marble contains two well developed joint sets. The dominant set strikes N 44° W and dips 60° southwest, with a subordinate set striking N 55° E and dipping 50° southeast. Both sets exhibit chlorite and iron oxide selvages, with chlorite being slightly more abundant along northwest trending joints.

Summary

Well-developed exsolution lamellae of dolomite exsolving from calcite are found in high-grade calcitic marbles. Exsolution is not observed in dolomite, indicating that the main period of dolomite formation occurred post-amphibolite-grade metamorphism.

Excellent preservation in talc of original marble layering and pseudomorphic textures such as serpentine after olivine with subsequent replacement of serpentine by talc, indicate constant volume replacement.

Structural control of talc formation is indicated by the localized nature of talc formation. Fluid movement was facilitated by joint and layering surfaces, evidenced by thin talc coatings on such surfaces. Any large structures which may have facilitated talc formation are no longer discernible.

SPRING CREEK PROSPECT

Introduction

The Spring Creek Prospect, controlled by CIMC, (Figure 2, SE 1/4 Sec. 32, T6S R6W) lies within the Regal Marble as named by Okuma (1971). Garihan (1973) mapped the Regal Marble in the prospect area as the overturned limb of a northeast trending, isoclinal synform. This

talc occurrence is within dolomitic marble, tens of meters from the nearest lithologic contact. Along strike from the prospect, this marble unit is largely calcitic, with dolomite found in significant amounts only within zones 10 m to 15 m from talc-bearing zones. Layering within marble is defined by talc lenses standing in positive relief on weathered surfaces, and strikes N 40-60° E, dipping 55-75° northwest. The geology of the prospect is shown in Plate 4.

High-Grade Marble

High-grade marble with intercalated tremolitic quartzite is found within 14 meters of the main talc body of the Spring Creek Prospect. This marble is generally coarse-grained, and contains the assemblage dolomite-olivine-phlogopite in the prospect area. Retrograde chlorite and tremolite are also present. Minor quartz is present as infillings of irregularly shaped vugs. Garihan (1973) also describes an assemblage of dolomite-diopside-tremolite-phlogopite-garnet-scapolite along strike in these marbles.

Equilibrium textures are not present in thin section. All chlorite examined is rutilated and appears to be an alteration product of phlogopite. Dolomite is fine-to medium-grained, and commonly twinned. Undulose extinction is absent in dolomite, patchy extinction is present but not well developed.

Talc-Bearing Marble

Talc-bearing marbles are white to buff (locally pink and maroon), medium-to coarse-grained, with the assemblage of dolomite-chlorite-talc-serpentine. Rare quartz and relict phlogopite and tremolite are

also present. Accessory minerals are pyrite, apatite, and graphite. Apatite is rare, and is present only within talc grains. The paragenetic sequence developed for the Spring Creek prospect is presented in Figure 8.

On hand sample and thin section scales dolomite is notably coarser-grained in talc-bearing marbles than in high-grade marbles. In thin section, patchy extinction is well developed, and indicates a minimum of two and probably three generations of dolomite. Twinning is present, but is less common than in high-grade marbles.

As in high-grade marbles, much of the chlorite present in talc-bearing marble is rutilated and is an alteration product of phlogopite (Table 2). Several phlogopite grains are present with a scaly texture caused by incipient exsolution of rutile.

Talc occurrences exhibit several distinct morphologies including: 1) a large layer-parallel body 1 m to 4 m thick with minor relict marble inclusions; 2) minor disseminated grains which locally occur as pseudomorphs after tremolite; 3) scattered, discontinuous coatings on layering and fracture surfaces; 4) minor centimeter-to meter-scale concordant and discordant irregularly shaped pods; and 5) millimeter-to centimeter-scale halos in marble surrounding chloritized and boudinaged biotite-quartz schist inclusions in marble.

The main talc body is a dominantly layer-parallel body 1 m to 4 m thick, which is discordant only near the lateral terminations of the body. Strike length of the talc body is unknown due to the presence of

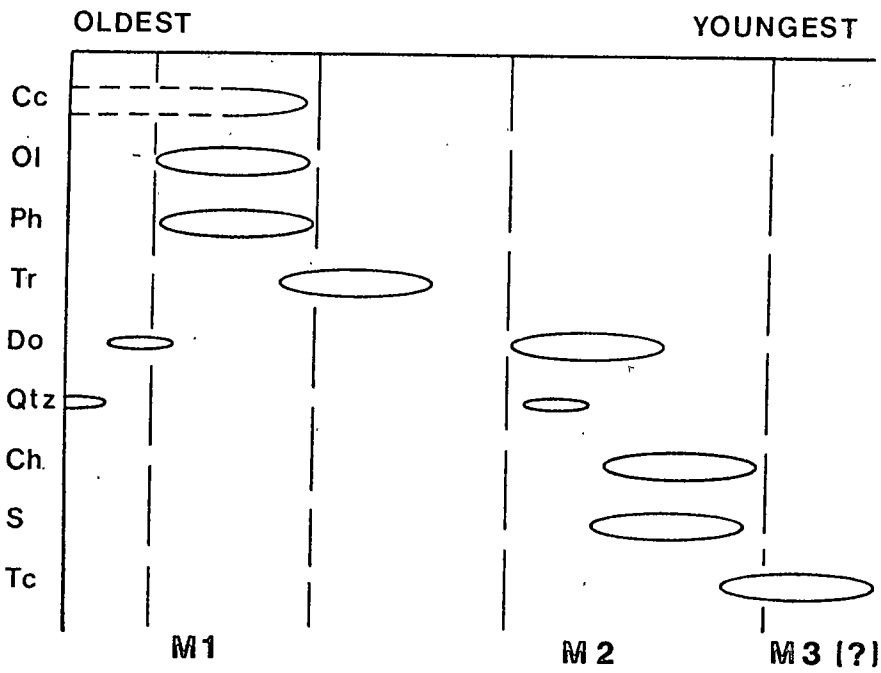

Figure 8. Diagram showing the paragenetic sequence for the Spring Creek Prospect.

debris overlying key exposures. This debris also prohibits determination of the nature of the lateral terminations of the talc body.

At the northeastern termination of the main talc body the basal talc-marble contact cuts abruptly upsection, causing the talc body to thin from 4 m thick to 1 m thick across a mine bench 9 meters wide (Plate 4). Assuming stratigraphic continuity across the bench, the projected equivalent of the truncated lower portion of the 4 meter thick talc body is a talc-rich zone composed of dense, coarse-grained dolomite, with up to 40 % talc in concordant and discordant pods. The reason for the lateral termination of the talc body is not obvious in outcrop.

In hand sample talc is dominantly light-to medium-green in color; however, there is also locally abundant maroon-to gray-colored talc, often with well developed leisigang banding. Pyrite, up to 5 mm in size, (partially or totally altered to hematite), and graphite are common accessory minerals in talc.

On a microscopic scale talc occurs as an alteration product of dolomite, phlogopite, serpentine, tremolite, and quartz. None of these reactions has gone to completion on thin section scale.

Quartz has altered to form talc in an apparently calcitic marble (Figure 9). Carbonate in contact with talc exhibits a different CL and UV signature than does ground mass carbonate, indicating sub-millimeter scale compositional variations between carbonates. Based on CL signatures, a fine rind of dolomite is inferred to be present immediately adjacent to talc. Preferential alteration of quartz to talc has been inferred at other prospects during this study; however, actual reaction fronts have not been observed. Alteration of quartz to talc has been reported elsewhere in the Ruby Range (Whitehead, 1979).

Rare, centimeter-to meter-scale biotite-quartz schist boudins within talc-bearing marble are oriented parallel to layering, and commonly exhibit crenulated, chloritized halos. Centimeter-scale talc halos are common in marble immediately adjacent to schistose boudins. Similar chlorite-talc relationships are seen in feldspar-quartz gneiss inclusions in marble at the Sweetwater Mine and in biotite schist inclusions in the Pope Prospect.

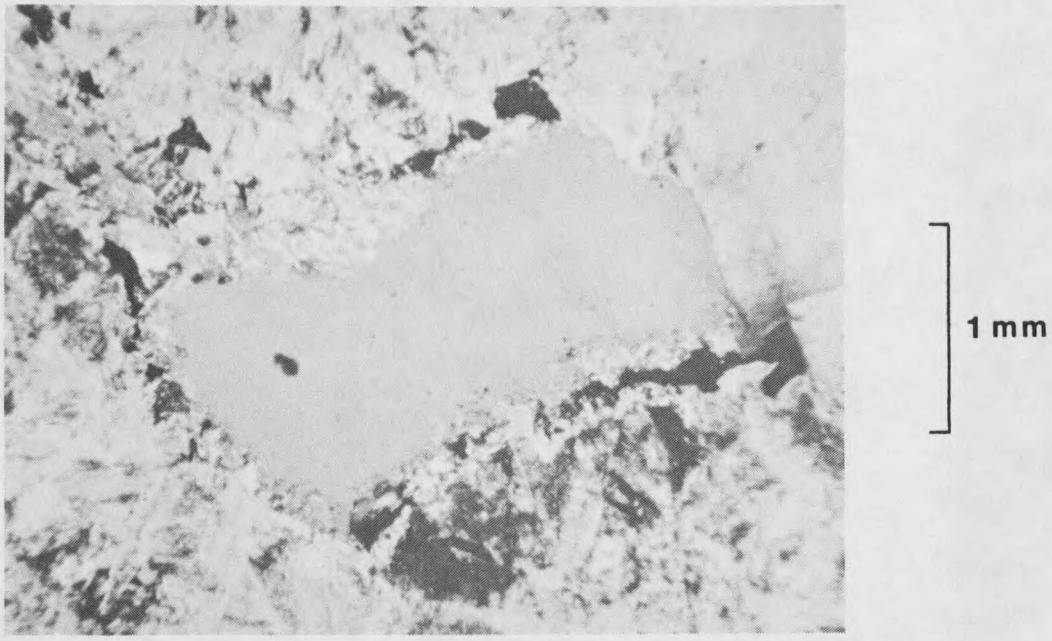

Figure 9. Photomicrograph showing quartz altering to form talc.

Structure

Detailed mapping has delineated several northwest-striking faults which dip steeply (>70 ^{o}) to the northeast and/or southwest (Plate 4). Most recent movement on all northwest trending faults post-dates talc formation, and is generally < 30 cm in total offset. Structures which may have provided conduits for talc forming fluids are not discernible at present. Also, no evidence is seen for fracturing or distortion of marble which can be genetically related to talc formation.

Summary

Carbonate-silicate relationships indicate multiple periods of mineral formation. Talc forms at the expense of dolomite, phlogopite,

tremolite, quartz, and serpentine. A very late-greenschist to post-greenschist age for talc formation is indicated.

The main talc body is a layer-parallel unit with a locally discordant basal contact. Evidence for movement of fluids which may have facilitated talc formation is rare, being marked only by scattered talc coatings on joint and layering surfaces.

Structural control of talc formation is indicated by the localized nature of talc formation. Cross-cutting structures which may have allowed fluid movement are not present.

Pope Prospect

Introduction

The area chosen for detailed study within the Pope claim block (held by CIMC) is the northwestern-most prospect pit, located in the NE 1/4 Sec. 12, T8S R7W (Figure 2). Calcitic to dolomitic marble in this prospect is intercalated with biotite-quartz-feldspar schists. Gneisses overlying and underlying the talc zone are identified as Dillon Gneiss (Okuma, 1971). Detailed geology of the propect is presented in Plate 5.

High-Grade Marble

High-grade marble is fine-to medium-grained, and contains the assemblage calcite-dolomite-olivine-diopside. Rare disharmonically folded quartz stringers are also present. Superimposed on the high-grade assemblage is a retrograde assemblage of serpentine-chlorite-tremolite.

The first appearance of high-grade marble is approximately 15 m west of the main talc body, and corresponds closely with an inferred, poorly defined alteration front in marble. This alteration front separates high-grade marble to the west from talc-bearing marble to the east, and is defined by westward decreasing dolomite content and grain size.

In thin section, scattered carbonate grains exhibit multiple periods of crystallization, evidenced by dolomite grains rimmed by later-formed calcite. Serpentine forms pseudomorphs after olivine. Tremolite occurs as pseudomorphs after olivine, as fine-grained acicular mats around olivine, and as discrete grains disseminated throughout the rock. Retrograde reactions did not go to completion on thin section scale.

Talc-Bearing Marble

Talc-bearing marble occurs within 3 meters of calcitic high-grade marble described above. Talc-bearing marbles contain a greenschist grade assemblage of dolomite-calcite-talc-serpentine. The paragenetic sequence determined for the Pope Prospect is presented in Figure 10.

Mining in the area has removed the main talc body. From talc left in place it is inferred that the talc body was formed within marble, at the contact of marble with overlying Dillon Gneiss. Overall, formation of talc disseminated in marble is restricted to a zone within 25 meters of the lithologic contact. This is the only occurrence of extensive talc formation at a lithologic boundary encountered during this study.

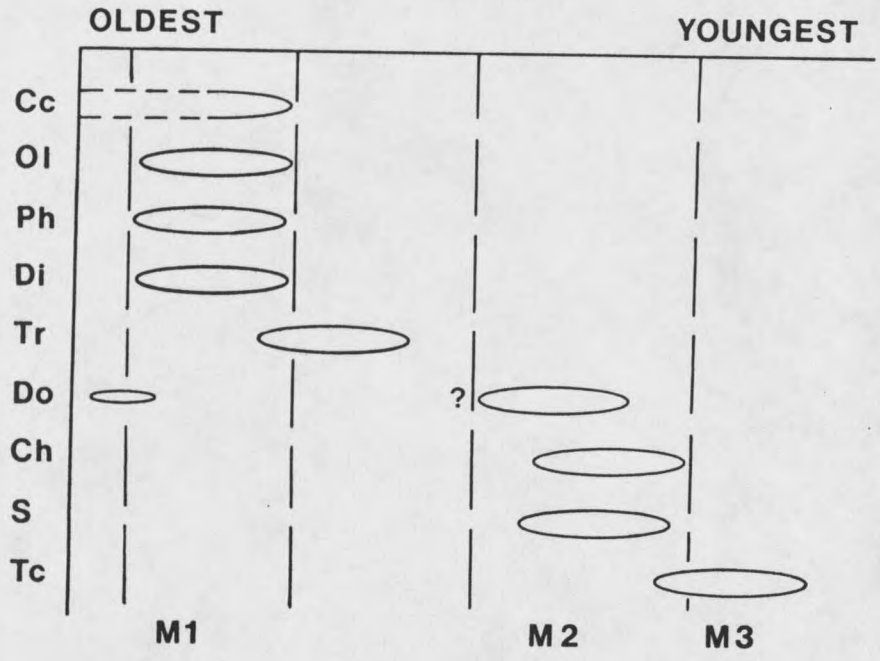

Figure 10. Diagram showing the paragenetic sequence for the Pope Prospect.

The amount of material removed indicates a talc body no more than 5 meters in thickness, with discontinuous lateral exposures indicating a strike length of about 60 meters.

In hand sample, talc commonly occurs as: 1) 1 cm-to 6 cm-thick halos in marble which surrounds the intercalated, chloritized schist bodies described below; 2) disseminated millimeter-to centimeter-scale blebs with botryoidal textures; 3) disseminated amorphous grains within marble; and 4) discontinuous coatings along layering planes.

In thin section talc exhibits several morphologies: 1) pseudomorphs after dolomite (Figure 11); 2) an alteration product of serpentine; 3) isolated, irregular pods, which commonly exhibit well-developed coronas of chlorite with minor serpentine (texturally similar

to talc ribbons in altered gneisses at the Sweetwater Mine); and 4) botryoidal grains within vugs lined by rhombohedral dolomite, with euhedral carbonate inclusions within talc.

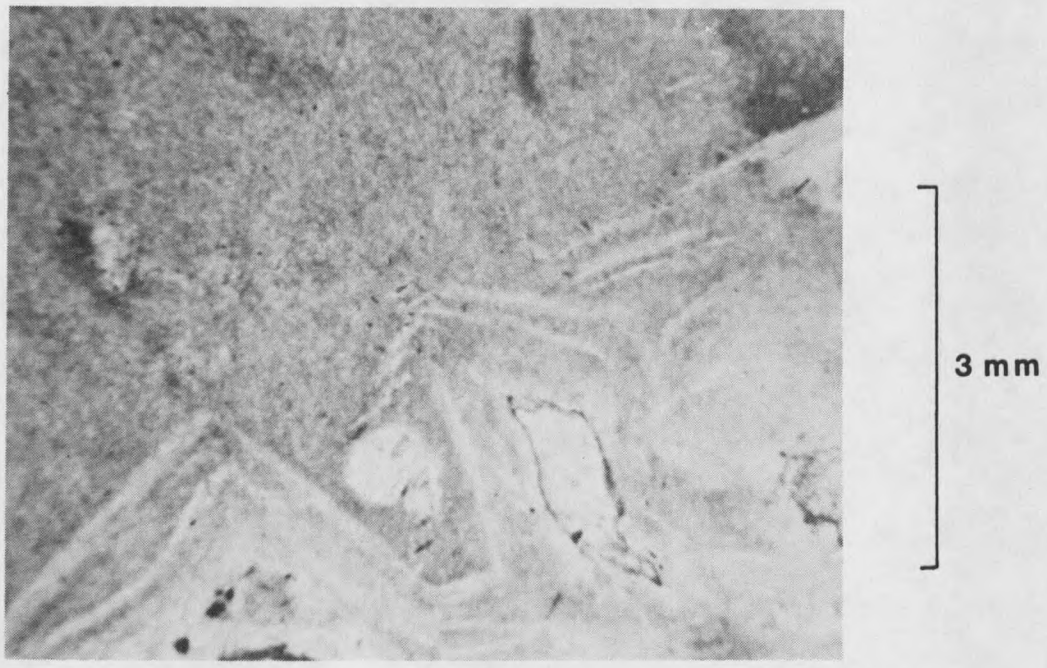

Figure 11. Photomicrograph showing talc pseudomorphs after dolomite, defined by color bands in talc (plane polarized light).

Schists

Schistose layers within talc-bearing marble have been isoclinally folded with axial surfaces parallel to foliation. In hand sample, retrograde chloritization of schists is expressed either as pervasive chloritization of schist lenses or as 6 cm-to 10 cm-thick chloritic selvages in schists where they are in contact with marble. Schists have been described by Okuma (1971) as possible altered ultramafic bodies. This interpretation seems unlikely based on mineralogic composition of the schists, which indicates a pelitic protolith.

On a microscopic scale, schists exhibit a fine-grained amphibolite-grade assemblage of plagioclase(An_{23-27})-K-Spar-quartz-biotite-garnet-sillimanite, with minor hematite. Retrogression to greenschist-grade is expressed by chloritization of garnet and biotite, and sericitization of plagioclase. Chlorite formed by alteration of biotite is commonly sagenitic. Fronts of pervasive greenschist alteration are expressed as sharp boundaries (1mm to 2 mm in width) across which the degree of alteration of biotite and garnet to chlorite changes from slight to intense.

One occurrence was noted of talc formation in schists. Blue-white talc is found as an apparent open-space filling along the nose of an isoclinally folded, pervasively chloritized schist body.

Dillon Gneiss

Rock immediately overlying the talc zone is identified as Dillon Gneiss (Okuma, 1971), which is moderately altered in hand sample. Chlorite selvages are common along joints striking N 30-40° W, dipping 70 - 80° southwest.

Summary

Amphibolite-grade assemblages in marbles and gneisses are overprinted by retrograde greenschist-grade assemblages. Fluid movement along lithologic contacts and layering planes in marble is indicated by chloritized rinds in schists, with talc halos forming in adjacent marble, and by discontinuous talc coatings on layering surfaces.

Structural control on talc formation is indicated by the restriction of talc growth to a relatively narrow zone adjacent to the marble-Dillon Gneiss contact.

Sweetwater Mine

Introduction

Mining has largely removed the main talc body in the Sweetwater Mine, held by CIMC, (Figure 2, Sec. 13 T8S R7W), preventing a detailed study of the major talc-forming reactions and mechanisms in this prospect. However, this prospect provides an opportunity to study well-exposed chloritic alteration in quartz-feldspar-garnet gneisses which are intercalated with magnesite-rich, talc-bearing marbles.

Marbles

High-Grade Marble. High-grade marble 20 m to 25 m northeast of the pit and 3 m to 4.5 m structurally below talc-bearing marble is gray-white, sugary, and contains contorted quartz stringers. An amphibolite-grade assemblage of dolomite-olivine-phlogopite has been overprinted by a greenschist-grade assemblage of serpentine-chlorite-tremolite. The paragenetic sequence for the marbles of the Sweetwater Mine marbles is presented in Figure 12.

Quartz occurs as contorted stringers, irregular pods, and as vug fillings. Irregular quartz pods are elongate in the plane of foliation and are commonly weakly boudinaged and deformed. Where quartz occurs as vug fillings, isolated, rounded carbonate grains are enclosed by quartz.

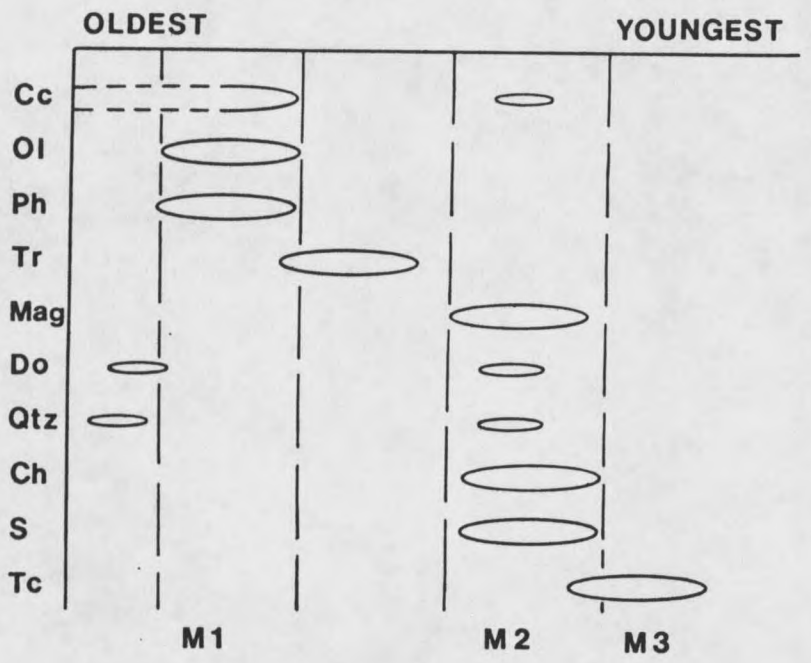

Figure 12. Diagram showing the paragenetic sequence developed for marbles at the Sweetwater Mine. M = magnesite.

Thin section examination reveals the presence of at least two generations of calcite. Smaller calcite grains exhibit well developed undulose extinction with rare patchy extinction. Larger calcite grains have less undulose extinction and common patchy extinction. These textural differences suggest incomplete recrystallization of calcite, with resultant release of strain and enlargement of grains.

Talc-Bearing Marble. Talcose marble within the pit is homogeneous, medium-to coarse-grained, friable, and composed largely of magnesite (presence of magnesite is not detectable optically, but is inferred on the basis of XRD analysis and whole rock geochemistry). Meter-scale gneiss inclusions which have been boudinaged and chloritized are common within talc-bearing marble.

Talc-bearing marbles contain the greenschist-grade assemblage magnesite-talc-chlorite. Evidence for equilibrium is lacking. Also present are dolomite, calcite, relict phlogopite, serpentine, minor tremolite, rare quartz, and accessory graphite and pyrite.

On a microscopic scale, magnesite is coarse-grained, with iron oxide staining common along cleavage traces. Where magnesite is in contact with talc, grain boundaries are irregular and jagged, indicating formation of talc from magnesite (Table 1).

Talc occurs as: 1) disseminated grains (pseudomorphous after serpentine and tremolite); 2) isolated pods; 3) open-space fillings; 4) centimeter-scale halos surrounding boudinaged gneiss inclusions; and 5) discontinuous coatings on layering surfaces.

Many talc pods occur as 1.25 cm to 4 cm lenses roughly parallel to layering, which appear to have been boudinaged and deformed. This texture is similar to that of quartz pods described in high-grade marble, suggesting preferential alteration of quartz to talc.

In thin section, relict textures in talc suggest that alteration of phlogopite, dolomite, serpentine and tremolite to talc is common. Other relict textures in talc are indeterminate in origin.

Meter-scale gneiss inclusions within marble exhibit both pinch-and-swell and chocolate block boudinage structures. Directions of extension for boudins are N 37° E and N 50° W, parallel to strike and dip of layering. Boudinaged gneiss is slightly to intensely chloritized, with abrupt, irregular alteration fronts between slightly and intensely chloritized gneisses. Dark gray to white talc-graphite rinds are present at all gneiss-marble contacts.

Gneisses

Introduction. Chloritization in gneisses appears to be cogenetic with talc formation in the intercalated marbles, and is preserved in increments from relatively unaltered gneiss to intensely altered gneiss. Although chloritic alteration of gneisses involves a slightly different chemical system than does alteration of dolomitic marble to talc, this prospect yields valuable information regarding physical mechanisms of chlorite formation which can be applied to talc formation in other areas examined during this study.

Unaltered Gneiss. Layering in relatively unaltered gneiss immediately north of the main pit strikes N 40-65° E and dips 35-50° NW. Oriented sillimanite locally defines foliation, as does a crude alignment of feldspar and rare quartz ribbons.

Relatively unaltered gneiss contains the amphibolite-grade assemblage plagioclase(An_{25-31})-orthoclase-garnet-sillimanite-quartz. Weak retrograde alteration of this assemblage is evidenced by formation of muscovite and sericite in plagioclase.

In thin section, garnet is rarely poikiloblastic, with inclusions of quartz and feldspar. No evidence for mechanical deformation of garnet is seen in thin section; however, in outcrop garnets are commonly crudely aligned along a mineral lineation trending N 15-20° E, and plunging approximately 23°. Sillimanite shows evidence of incipient alteration, but the alteration product is not identifiable optically.

Slightly Chloritized Gneiss. Within the main pit, unaltered gneiss grades into a slightly chloritized gneiss with moderately

abundant northwest-striking, northeast-dipping joints. Moderate to pervasive chloritic replacement of feldspar characterizes alteration along these joints.

On a microscopic scale, slightly chloritized gneiss contains the assemblage plagioclase-orthoclase-quartz-sillimanite, with retrograde chlorite, sericite, and muscovite. Quartz and feldspar grains are seen to have coalesced into ribbons up to 6mm in length. Sillimanite is present as intensely altered elliptical clots. Groundmass sericite, formed from alteration of plagioclase, often exhibits crudely defined grain boundaries, apparently mimicking relict feldspar grains. Relict garnet porphyroblasts are defined by chlorite enclosing sericite, muscovite, quartz and feldspar.

Intensely Chloritized Gneiss. Pervasive chloritic alteration (and talc formation) is restricted to stratigraphic horizons exposed within the main pit. Weakly chloritized gneiss changes abruptly to intensely chloritized gneiss across irregular alteration fronts 0.5 centimeters or less in width.

Intensely chloritized gneisses contain the assemblage chlorite-talc-serpentine-brucite (?). In thin section, chlorite occurs as a replacement of sericite (after feldspar). Talc, formed by preferential alteration of quartz ribbons, is commonly separated from the chloritic groundmass by moderately well developed coronas of serpentine and brucite (?)(Figure 13).

Relict gneissic textures are locally well preserved in intensely chloritized gneiss. Figure 14 shows a common relict texture, in which

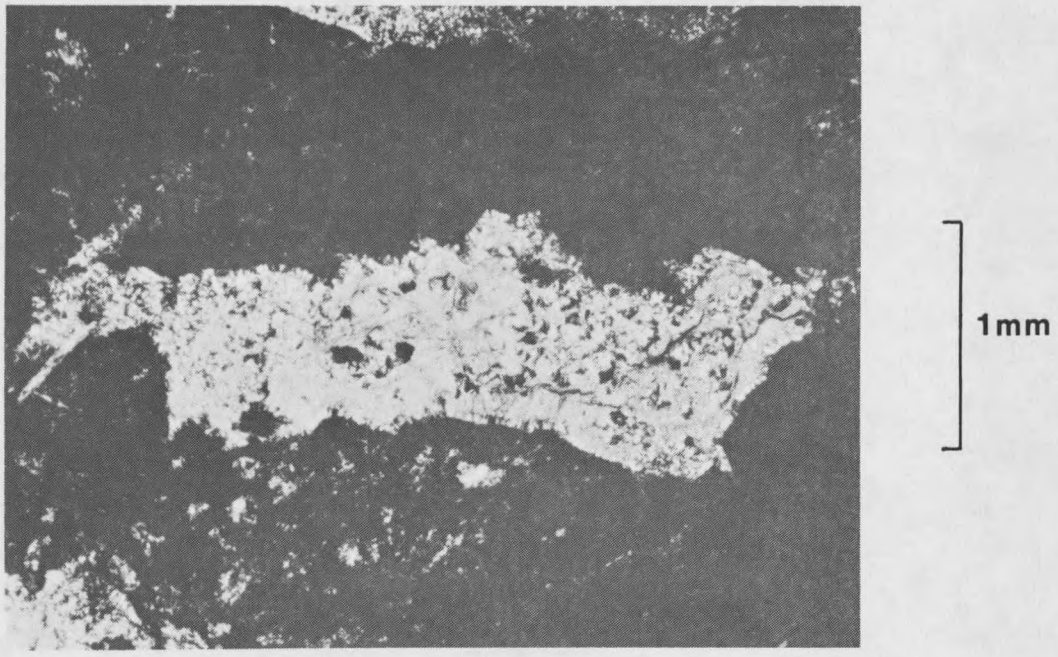

Figure 13. Photomicrograph showing relict quartz ribbons which have been altered to talc, surrounded by chloritized feldspar. Note serpentine-brucite (?) halo.

Figure 14. Photograph of relict gneissic texture in which quartz ribbons preferentially altered to talc wrap around a chloritized feldspar porphyroblast.

quartz ribbons, selectively altered to micaceous talc, wrap around a feldspar porphyroblast which is completely altered to chlorite.

Structure

Two joint sets are present in the area. The first strikes N 40-60° W, dips 55-65° northeast, and exhibits pervasive chloritization along joint surfaces, with chlorite locally flooding into adjacent gneiss. The second joint set, less well developed than the first, strikes N 75° E and dips 60° southeast. Iron oxide alteration dominates along these joints, but does not extend into neighboring gneisses.

Discussion

Mineralogic and Textural Relationships

Data presented in previous sections show that all prospects examined have similar paragenetic histories. Three periods of crystallization, M_1, M_2, and M_3 are indicated.

High-grade marbles are characterized by the amphibolite-grade (M_1) assemblage calcite-olivine-phlogopite +/- dolomite. Secondary quartz is also present, as disharmonically folded stringers and as vug fillings. M_1 is commonly overprinted by retrograde mineralization (M_2), characterized by dolomite-chlorite-serpentine.

Talc-bearing marbles typically contain a greenschist-grade (M_2) assemblage of dolomite-chlorite-serpentine +/- calcite, overprinted by formation of talc (M_3). Tremolite, relict phlogopite, and rare quartz are also present. Evidence for equilibrium assemblages is lacking.

Calcite and dolomite in talc-bearing marbles exhibit textures indicating a complex crystallization history. Exsolution textures in carbonates show dolomite exsolving from calcite, indicating that marbles were calcitic during amphibolite-grade metamorphism, with the main period of dolomitization occurring after amphibolite-grade metamorphism. This is consistent with field observations indicating that high-grade marbles tend to be calcitic, with talc-bearing marbles tending to be dolomitic. It should be noted that at least a small amount of dolomite was present early in the history of the marbles, acting as the source for Mg^{++} to form olivine, diopside, and phlogopite.

The last stage in the paragenetic sequence, M_3, is marked by localized recrystallization of dolomite, phlogopite, tremolite, quartz, magnesite, and serpentine to form talc. The observation that talc is nowhere seen recrystallizing to form other phases leads to the supposition that talc formation is the last major event in the paragenetic history of marbles examined.

Formation of talc from dolomite should result in the formation of by-product calcite (Table 2). Using normal petrographic observations, and CL and UV microscopy, calcite which might be cogenetic with talc formation has not been differentiated, nor has such a calcite population been identified on outcrop scale. This observation is consistent with previous studies (Garihan, 1973; Berg, 1979; Piniazkiewicz, 1984), and suggests that calcite which is cogenetic with talc formation may have been removed from the system.

Excellent preservation of relict textures in marbles and gneisses indicates that talc formation occurred under static conditions, and

that constant volume relationships were maintained. Examples of such features in marbles include locally abundant pseudomorphs of talc after dolomite, tremolite, and serpentine. Relict textures are also well preserved in moderately to intensely altered gneisses which occur as boudins within marbles and as discrete lenses intercalated with marbles.

Structural Control of Talc Formation

Field and petrographic evidence suggests that talc formation is largely structurally controlled. With the exception of small northwest trending joints, very few cross-cutting structures demonstrate evidence for fluid movement which may be related to talc formation. This observation, combined with the dominantly layer-parallel nature of larger talc bodies (which are locally discordant) suggests that observed talc formation may have been controlled by discontinuous layer-parallel fractures. Talc formation may then be explained by irregular fluid movement along layer-parallel fractures which caused little or no visible offset in marbles. It should be noted that the podiform nature of many of the dolomitic zones noted during field mapping may also be explained by Mg^{++}-rich fluid movement along such structures prior to formation of talc.

Areas with abundant talc examined during this study are generally surrounded by zones of retrograde greenschist mineral formation, which are in turn surrounded by high-metamorphic grade assemblages. These relationships suggest that discrete localitites within continuous marble bands experienced brittle fracturing after amphibolite-grade

metamorphism, thus forming pathways for fluid migration during subsequent retrograde recrystallization and talc formation.

Pathways for fluid movement during talc formation are evidenced by discontinuous talc-chlorite coatings and centimeter-scale halos surrounding layering surfaces, joints, and marble-gneiss lithologic boundaries. It should be noted that major structures that may have provided conduits for fluid movement were not identified as part of this study.

Stratigraphic Controls on Talc Formation

The possibility exists that pre-talc compositional variations between marble layers may have played an important role in formation of massive talc bodies, with talc forming by preferential alteration of favorable horizons. Such stratigraphic control would result in layer-parallel (or nearly so) talc bodies. It is felt that this hypothesis can be largely discounted due to the nature of lateral pinch-outs of talc bodies. If talc formation was controlled by stratigraphic compositional variations, discordant lateral terminations would not be expected. It is important to note that even though this mechanism is not favored for formation of large layer-parallel bodies, it may have some validity on a smaller scale. Preferential alteration of quartz rich stringers to talc is suggested by similarities in the morphology of folded quartz stringers in high-grade marble, and contorted talc stringers in talc-bearing marbles.

The above discussion shows that, by itself, stratigraphic compositional variation is not the favored mechanism for control of

talc formation. However, talc formation may have occurred along certain compositional horizons which contained fractures that cross-cut layering at a low angle, resulting in layer-parallel talc bodies with discordant terminations.

CHAPTER 3

WHOLE ROCK GEOCHEMISTRY

Introduction

Examination of the whole rock geochemistry of high-grade marble (HGM), talc-bearing marble (TBM) and talcose bodies provides data useful in determining the nature of bulk-compositional changes in marbles resulting from talc formation. Trends defined on the basis of geochemistry are consistent with microscopic-scale textural relationships, and allow interpretations to be made concerning the mechanism of talc formation.

Data

Twenty-seven samples of HGM, TBM, and talc were collected for whole rock geochemical analysis using X-Ray Fluorescence (XRF). Where appropriate, samples of altered gneiss immediately adjacent to marbles and/or talc were also examined to determine if the nature of alteration within gneisses coincides with that seen in marbles. The results of marble and gneiss analyses are presented in Appendix 1. Analyses for HGM, TBM, and talc are shown on a ternary CaO-MgO-SiO_2 diagram in Figure 15.

Discussion

As shown in Figure 16, HGM, TBM, and talc occupy distinct fields with little, if any, overlap between fields. Two distinct trends are suggested, denoted by arrows in the diagram, that indicate the path of talc petrogenesis.

The first trend noted marks the transition from HGM to TBM. In the HGM/TBM transition an increase in MgO is apparent, marked by increased MgO/CaO ratios, with little apparent mobilization of SiO_2. Also, examination of the relationship between MgO/SiO_2 isopleths (lines of equal composition) and the fields of HGM and TBM in Figure 16 shows that the MgO/SiO_2 ratio increases slightly in response to the relative increase of MgO in the system. These relationships are interpreted as the result of dolomitization having occurred after amphibolite-grade metamorphism (with possible coeval formation of magnesite at the Sweetwater Mine). This interpretation is in agreement with microscopic-scale carbonate textures (dolomite exsolving from calcite) which indicate that marbles tended to be calcite-rich at the time of high-grade metamorphism.

The second trend delineated marks the transition from TBM to talc. The TBMs are initially dolomite-rich, and are seen to follow a trend from a bulk composition near dolomite to a bulk composition of pure talc. The SiO_2/MgO ratio increases systematically within the TBM field, suggesting introduction of large quantities of SiO_2 to form talc from TBM (assuming a homogeneous dolomitic precursor). This interpretation suggests that the fluid phase controlled the mineralogy

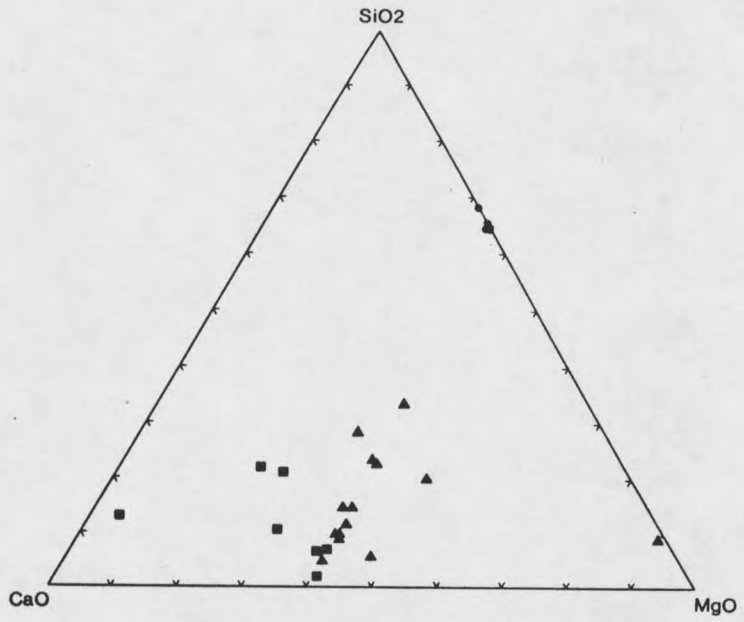

Figure 15. CaO-MgO-SiO_2 ternary diagram showing high-grade marbles (squares), talc-bearing marbles (triangles), and talc (circles).

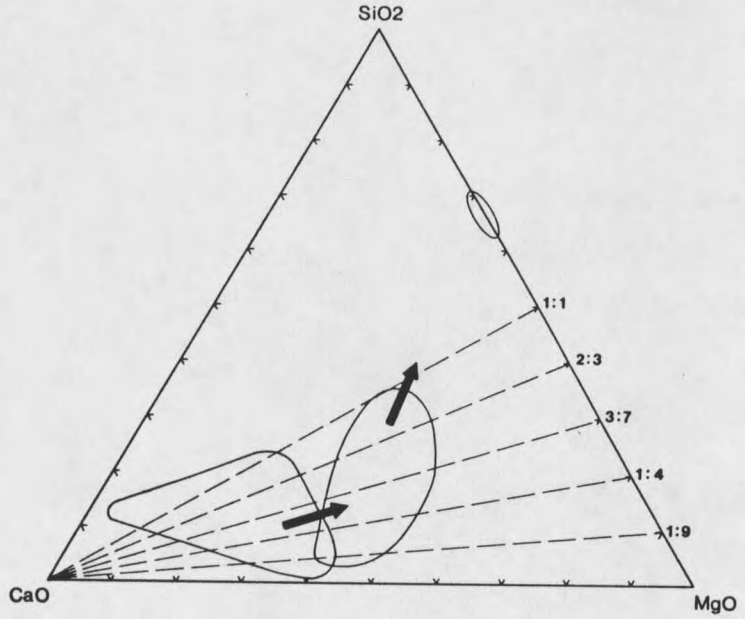

Figure 16. CaO-MgO-SiO_2 ternary diagram showing fields occupied by HGMs, TBMs and talc. Arrows denote trends between HGMs, TBMs and talc. SiO_2/MgO isopleths radiate from the CaO pole to the MgO-SiO_2 tie line.

of the system during talc formation by the process of infiltration (Rice and Ferry, 1982), with the amount of introduced SiO_2 acting as the limiting component of talc formation from precursor dolomitic marble. This interpretation is similar to conclusions drawn during previous studies (Okuma 1971; Garihan, 1973; Olson, 1976; Berg, 1979). Microscopic-scale observations are in agreement with this interpretation in that: 1) isobaric univariant mineral assemblages have not been observed, thus indicating that mineralogic buffering of the fluid phase has not occurred; and 2) visual estimates of talc present in TBM on a microscopic scale increases as percentage of SiO_2 increases, with free quartz rarely being present in TBMs.

It is interesting to note that the slope of the trend from TBMs to talc crosses MgO/SiO_2 isopleths at a relatively high angle, in contrast to the approximately parallel trend line-isopleth relationship noted for the HGM/TBM transition. These relationships suggest the possibility that two periods of fluid flux occurred. Alternatively, differing MgO/SiO_2 ratios may have resulted from gradational compositional changes during a single period of ongoing fluid flux, which affected the transition from HGM to TBM, followed by the transformation of TBM to form talc.

A third possible trend, the direct transition of HGMs to talc, is not considered due to lack of macroscopic and microscopic evidence supporting such an interpretation.

Geochemistry of Gneisses

With one exception, whole rock chemistry of altered gneisses is ambiguous with respect to determination of the nature of fluids which caused the observed alteration. The one exception noted is that of the Sweetwater Mine, where intensely chloritized gneisses are intercalated with magnesite-rich TBM. Analyses of relatively fresh, slightly altered, and intensely altered gneiss are presented in Appendix 1. Efforts were made to insure that samples were taken from the same stratigraphic horizon to minimize chemical variations caused by compositional layering.

Chemistry of gneisses from the Sweetwater Mine indicates that approximately one-half of the total SiO_2 present in the least altered gneisses was removed during transformation to intensely chloritized gneiss, and that substantial quantities of Mg^{++} were added. These changes result in an end-product of gneisses which have a bulk composition identical to that of chlorite.

The mechanism which affected chloritization of gneisses may also explain the mineralogy of intercalated magnesite-talc marbles. Chloritization of gneisses resulted from addition of Mg^{++} to the system under greenschist-grade conditions. This Mg^{++} enrichment may explain coeval magnesite formation in adjacent marbles. Chloritization of gneisses resulted in SiO_2 depletion in gneisses, which would then be available for talc formation in adjacent marbles by the process of mass transfer across lithologic boundaries. If MgO is present in excess, as suggested by the presence of chlorite and magnesite, it would appear

that SiO_2 is the limiting component of talc formation in this prospect. This interpretation is consistent with interpretations of talc formation in other prospects examined, with the major difference being the Mg^{++}-rich nature of the fluids which brought about the observed mineralization.

CHAPTER 4

MASS BALANCE

Introduction

Mass balance calculations can be used to model talc formation in closed or open systems. These calculations result from the determination of the nature of the talc-forming system examined here (open or closed). The calculations are further predicated on field and petrologic observations, and address the nature of changes in the mass and volume of the system which resulted from talc formation. These results, used in conjunction with phase equilibria, allow talc-forming fluids to be characterized to the greatest extent possible with the methodology of this study.

Mass balance calculations presented here will only address the alteration of dolomite to form talc by the reaction:

$$3\ \text{Dolomite} + 4\ \text{Quartz} + 1\ H_2O = 1\ \text{Talc} + 3\ \text{Calcite} + 3\ CO_2 \quad (1).$$

This limitation is imposed for several reasons: 1) alteration of dolomite is by far the most common reaction contributing to talc formation (this observation is consistent with previous studies); 2) the complexity of the over-all talc-forming system (six phases are identified as having contributed to talc formation); and 3) microprobe

data allowing exact determination of mineral compositions, necessary for calculations involving more complex phases and solid solution, is lacking.

Isochemical Talc Formation

Whole rock geochemical analyses of HGMs and TBMs are examined in terms of normative mineralogy (Talc, Dolomite and Calcite) to determine whether talc formation as observed in this study can be explained by isochemical alteration of HGMs and/or TBMs. Normative mineral determinations for HGMs and TBMs are presented in Tables 3 and 4 respectively.

From examination of Tables 3 and 4 it is clear that isochemical alteration of HGMs and/or TBMs does not result in formation of pure talc. It should be noted that normative weight percent determinations are anomalously high given the initial average bulk chemistry. High normative percentages result from normalizing SiO_2, MgO, and CaO prior to calculating molecular proportions to be used in normative calculations. These increases result from high Lost On Ignition (LOI) values inherent in analysis of carbonate rocks. By inspection it is seen that values for SiO_2, MgO, and CaO in HGMs are increased 37 %, with corresponding TBM values increasing 42 %, resulting in anomalously high normative values. Final normative mineral percentages are multiplied by the total average analysis, 63 % for HGMs and 58 % for TBMs, to adjust for high LOI values.

Adjusted normative percentage of talc in TBMs is compatible with visual percentage estimates determined in thin section. Given the

Table 3. Normative mineralogy of high-grade marble, calculated in terms of talc, dolomite, and calcite. See text for discussion.

High-Grade Marble Normative Mineralogy (defined in terms of Dolomite (Do), Talc (Tc), and Calcite (Cc)).

Avg. Geochemical Analyses:	Mol. Proportions:
SiO_2: 7.07 %	SiO_2: 0.187
MgO: 21.19 %	MgO: 0.834
CaO: 34.80 %	CaO: 0.984

1) Assign all SiO_2 to talc. Add MgO in 3:4 ratio.

   a) 0.187 (Tc) x 0.75 = 0.140 (MgO); leaves 0.694 MgO

2) Assign all excess MgO from 1a to Do. Add CaO in 1:1 ratio.

   a) 0.694 (MgO) + 0.694 (CaO); leaves 0.290 CaO

3) Assign all excess CaO from 2a to Cc.

   a) 0.290 (Cc)

Total Normative minerals (in weight %)	Adjusted Normative % (Total Normative x 0.63)
Talc = 31.18 %	Talc = 19.74 %
Dolmite = 56.15 %	Dolomite = 35.37 %
Calcite = 12.74 %	Calcite = 8.02 %
Total 100.07 %	LOI = 37.00 %
	Total 100.13 %

Isochemical alteration of an average HGM to form talc would result in formation of no more than 20 % talc.

Table 4. Normative mineralogy of talc-bearing marble, calculated in terms of talc, dolomite, and calcite. See text for discussion.

Talc-Bearing Marble Normative Mineralogy (defined in terms of Dolomite (Do), Talc (Tc), and Calcite (Cc)).

Avg. Geochemical Analyses:	Mol. Proportions:
SiO_2: 9.56 %	SiO_2: 0.274
MgO: 23.28 %	MgO: 0.995
CaO: 25.20 %	CaO: 0.774

1) Assign all SiO_2 to talc. Add MgO in 3:4 ratio.

   a) 0.274 (Tc) x 0.75 = 0.206 (MgO); leaves 0.789 MgO

2) Assign all excess MgO from 1a to Do. Add CaO in 1:1 ratio.

   a) 0.789 (MgO) + 0.774 (CaO); CaO deficient, leaves 0.15 excess MgO

3) Assign all excess CaO from 2a to Cc.

   a) CaO deficient, no Cc

Total Normative Minerals (in weight %)	Adjusted Normative % (Total Normative x 0.58)
Talc = 41.13 %	Talc = 23.85 %
Dolomite = 56.48 %	Dolomite = 32.75 %
Calcite = 0.00 %	Calcite = 0.00 %
Excess MgO = 2.39 %	Excess MgO = 1.38 %
Total 100.00 %	LOI = 42.00 %
	Total 99.98 %

Isochemical alteration of an average TBM to form talc would result in formation of no more than 24 % talc.

---

similarity of average SiO_2 content in TBMs and HGMs, normative values for talc in HGMs is considered reasonable.

It is important to note that in both HGMs and TBMs SiO_2 is the limiting component with respect to talc formation (i.e., dolomite is present in excess in both cases). This is consistent with interpretations based on geochemical data in this study and with interpretations of previous studies (Okuma, 1971; Garihan, 1973; Olson, 1976; Berg, 1979).

Metasomatism and Talc Formation

Normative mineralogy of HGMs and TBMs, and geochemical data indicate that talc formation must have occurred in an open system with metasomatic introduction of SiO_2. Calculations presented in Table 5 examine talc formation in dolomitic marbles deficient in SiO_2, with Mg^{++} held constant. Dolomitic marble composition is assumed on the basis of petrographic observations and geochemistry which indicate that the main period of dolomite formation post-dated high-grade metamorphism, and preceded talc formation. SiO_2 deficiency is assumed on the basis of geochemistry and field observations indicating low initial SiO_2 content in HGMs and TBMs.

As previously described (Chapter 1), by-product calcite which should have formed from alteration of dolomite to talc has not been recognized as part of this study, nor has calcite having this origin been noted in previous studies (Garihan, 1971; Piniazkiewicz, 1984). Lack of calcite which is cogenetic with talc formation suggests that

Table 5. Mass balance calculations holding Mg^{++} constant and introducing all SiO_2 and H_2O necessary to form talc from 1 m^3 of dolomitic marble. Note 29 % volume loss due to expulsion of calcite.

Hold Mg^{++} constant during alteration of one cubic meter (1 m^3) of dolomite (Do) to form talc (Tc) and calcite (Cc) by Reaction 1. Assume introduction of all SiO_2 and H_2O necessary to alter marble completely to talc and calcite (all molar volumes and formula weights used are taken from Robie and others (1978)).

Given: 1) 1 m^3 = 1 x 10^6 cm^3
2) Molar Volume of Do = 64.34 cm^3
3) Molar Volume of Tc = 136.25 cm^3
4) Molar volume of Cc = 36.93 cm^3
5) Molar volume of SiO_2 = 22.688 cm^3
6) Formula weight of Do = 184.403 g
7) Formula weight of SiO_2 = 60.085 g
8) Formula weight of Tc = 379.268 g
9) Formula weight of Cc = 100.089 g
10) SiO_2 is present in a 4:3 ratio with Do

1 m^3 Do = 15,542 moles Do.

15,542 moles Do, combined with 20,723 moles SiO_2 yields 5,181 moles of Tc and 15,542 moles of Cc (by stoichiometry of Reaction 1).

Mass of SiO_2 added is 1,245 kg.

5,181 moles Tc occupies a volume of 705,885 cm^3, 71 % of the original volume. Mass of Tc produced is 1,965 kg.

15,542 moles of by-product Cc occupies a volume of 547,028 cm^3, 57.4 % of the original volume of 1 m^3. Mass of Cc produced is 1,556 kg.

Complete alteration of dolomite to form talc (Tc) with concomitant removal of by-product calcite would result in a net volume loss of 29 %.

---

calcite was totally removed from the system. The net volume loss described in Table 5 reflects this assumption.

From Table 5 it is seen that alteration of 1 m^3 of dolomitic marble to form talc with SiO_2 and H_2O added in excess, and with all by-product calcite removed from the system, will result in formation of

talc which will occupy 29 % less volume than the original 1 m^3 of dolomite. The mass of SiO_2 added to the system is 1,245 kg, masses of talc and calcite formed are 1,965 kg, and 1,556 kg respectively.

Field observations indicate that talc formation by the mechanism presented in Table 5 is unlikely for two reasons. First, formation of chlorite blooms in gneisses adjacent to TBMs is interpreted to be coeval with talc formation, indicating that Mg^{++} was not held constant during the talc forming event. Second, constant volume conditions during talc formation are indicated by field and petrographic observations, in that: 1) deformation related to talc formation was not observed during field mapping; and 2) relict textures and pseudomorphs are preserved in marbles (and intercalated chloritized gneisses).

Given the criteria above, talc formation will now be considered from a constant volume standpoint. Calculations for a constant volume case are presented in Table 6.

The largest problem to be overcome in considering constant volume talc formation is the 29 % volume loss resulting from expulsion of calcite from the system. However, constant volume could be maintained in such a situation if SiO_2 and Mg^{++} were available in solution in excess of amounts necessary to completely alter dolomite to talc, and were precipitated to form talc in open spaces. This supposition is supported by field and petrographic observations of talc occurrences as open-space fillings.

Calculations presented in Table 6 show that, for volume to be conserved during alteration of one cubic meter of dolomite to form talc, 1,764 kg SiO_2 and 157 kg Mg^{++} must be introduced, resulting in

Table 6.3 Calculations showing total mass of SiO_2 and Mg^{++} added to 1 m^3 of dolomitic marble to conserve volume while altering marble completely to talc.

Given: 1) Assume original volume of dolomitic marble = $1m^3$
2) Molar volume of Tc = 136.25 cm^3
3) Formula weight of Talc = 379.268 grams (g)
4) Formula weight of SiO_2 = 60.085 g
5) Formula weight of Mg^{++} = 24.305 g

5,181 moles Tc = 71 % of the volume of 1 m^3 (from Table 5). This requires an additional 2159 moles of talc to form from introduced SiO_2 and Mg to maintain constant volume.

Multiplying 2,159 moles of talc by subscript values in the idealized talc formula for SiO_2 and Mg^{++} allows determination of the number of moles of each which was introduced into the system to maintain constant volume. These values can then be multiplied by their respective atomic weights to determine total weight of material introduced to maintain constant volume.

It must be remembered that, to determine total mass of material introduced to the system, the amount of SiO_2 necessary to alter the original $1m^3$ of dolomite to talc must also be accounted for. From Table 5, this value is 20,723 moles of SiO_2.

SiO_2: 2,159 moles x 4 = 8,635 moles
8,635 moles x 60.085 g/mole = 518.83 kg added to system

Mg^{++}: 2,159 moles x 3 = 6,476 moles
6,476 moles x24.305 g/mole = 157.4 kg added to system
Original SiO_2: 20,723 moles x 60.085 g/mole = 1,245 kg

Total SiO_2: 519 kg + 1,245 kg = 1,764 kg added to system

---

formation of talc and calcite with a total mass of 4,340 kg (with 1,556 kg of calcite having been removed). Thus, total solids introduced during talc formation comprise approximately 45 % of total solids present after formation of talc is complete (with calcite being removed from the system).

Estimates on Fluid Flux During Talc Formation

Given the total mass of silica added to the system during talc formation (Table 6), and the solubility of SiO_2 at the temperature (T) and pressure (P) of interest (from Chapter 6, 400° and 2 kbar), estimates can be made of the fluid flux necessary to introduce this quantity of SiO_2. Experimental and theoretical work on SiO_2 solubility by Morey and Hesselgesser (1951), Wood (1958), and Weill and Fyfe (1964) are in relatively good agreement, and indicate a maximum solubility of SiO_2 (as quartz) in H_2O of approximately 0.25 weight percent at the T and P noted above. The minimum fluid volume required to introduce 1,764 kg SiO_2 at a concentration of 0.25 weight percent is 705,600 liters. It should be noted that, at lower T and/or P the maximum solubility of SiO_2 decreases, thus increasing the fluid flux necessary for SiO_2 introduction. For example, at 300° C and 1 kbar, the maximum solubility of SiO_2 is 0.09 weight percent, which would require a fluid flux of 1.96×10^6 liters to introduce 1,764 kg SiO_2.

Discussion

Normative mineralogy of HGMs and TBMs indicates that talc formation as observed during this study could not result from isochemical alteration of HGMs and/or TBMs. Metasomatism is thus indicated as the mechanism which effected talc formation.

Several approaches to mass balance calculations are possible, with the best-fit case being constrained by field observations. The possibility that Mg^{++} was held constant during talc formation, thus controlling other extensive parameters of the system, must be

considered. This case results in a net loss of volume of 29 % after calcite removal is considered. A net volume loss and constant Mg^{++} are not consistent with field relationships indicating that talc formed under constant volume conditions, nor with chloritization of gneisses (interpreted to be coeval with talc formation) in close proximity to talc bodies. Also, the constant Mg^{++} case does not adequately explain occurrences of talc as an open-space filling. Talc formation under conditions which meet constant volume criteria is the preferred case.

Mass balance calculations based on conservation of volume are preferred due to preservation of relict textures, volume for volume (pseudomorphic) replacement of dolomite and other phases, and a lack of deformation of marbles or adjacent gneisses related to talc formation. Also, the constant volume case presented may explain formation of talc as an open-space filling, after considering volume loss due to calcite removal.

Implications of Mass Balance Calculations

Mass balance calculations clearly indicate that large volumes of SiO_2, Mg^{++} and H_2O from external sources must have moved through each volume of dolomitic marble altered to talc. A large external reservoir is indicated for SiO_2, Mg^{++} and H_2O.

A net loss of calcite from the system is assumed based on field observations, and, as previously stated, a sink for this calcite has not been noted from field or petrographic observations. It is possible that calcite was removed from the system by the same fluids responsible for influx of SiO_2 and Mg^{++}. Mass balance calculations show that

removal of calcite contributes greatly to the total mass of SiO_2 and Mg^{++} which must be added to the system to occupy the volume evacuated by calcite.

Sources of Silica and Magnesium

Chlorite pods in gneiss surrounding talc-bearing marbles may have provided a source for at least part of the SiO_2 necessary for talc formation. Such a relationship is problematic due to lack of evidence concerning timing of chlorite formation relative to talc, and the lack of data regarding the amount of SiO_2 liberated during formation of chlorite pods. It is doubtful however, that isolated occurrences of chlorite could have provided SiO_2 in quantities indicated by mass balance calculations.

Chlorite pods in gneiss surrounding talc-bearing marbles compound the problem of a source for Mg^{++}, in that Mg^{++} must have been added to gneisses to accomodate chlorite formation. Chlorite formation therefore could not provide any of the Mg^{++} which has been shown to have been added to marbles.

Mafic dikes may have contributed Mg^{++} to marbles. However, mafic dikes do not exhibit alteration consistent with Mg^{++} depletion (Wooden and others, 1978). Further, in all but one prospect examined mafic dikes are not spatially related to talc-bearing marbles. Lack of alteration and spatial relationships combine to make this an unlikely mechanism.

Meteoric water is a potential source for material added during talc formation, given the shallow depth of talc formation which has

been proposed. Meteoric waters associated with hot springs and other hydrothermal systems are commonly enriched in SiO_2 (Ellis and Mahon, 1977). The source of Mg^{++} in such waters is again a problem, given that such systems are not noted for enrichment in Mg^{++}. Also, gneisses surrounding talc-bearing marbles are a relatively poor source rock for leaching of Mg^{++} by meteoric waters, based on mineralogy described in previous studies (Garihan, 1971; Okuma, 1973). Meteoric water should be considered as a source of fluids for talc formation even though a source of Mg^{++} is lacking.

CHAPTER 5

RELATIVE AND ABSOLUTE AGES OF TALC FORMATION

Relative Age of Talc Formation

The relative age of talc formation has been established as very late-to post-greenschist-grade metamorphism (Chapter 2). Based on mineralogic relationships this relative age can not be further refined, that is, it can not be determined wether or not talc formation is a distinct and separate event which totally post-dates Proterozoic greenschist-grade thermal metamorphism.

Absolute Age of Talc Formation

Regional geologic studies indicate that the Ruby Range experienced lower-granulite to upper-amphibolite-grade metamorphism, dated at 2750 Ma., with subsequent retrograde greenschist thermal metamorphism dated at 1600 Ma. (Gilletti, 1966; James and Hedge, 1980). Serpentine present in talc-bearing marbles probably represents incipient greenschist-grade thermal metamorphism.

Serpentine-talc phase relationships (Figure 17) indicate that a thermal pulse must have accompanied recrystallization of serpentine to form talc after the amphibolite-grade metamorphic event described above. Examination of possible causes of such thermal pulses helps to place formation of economically viable talc bodies in an absolute time framework.

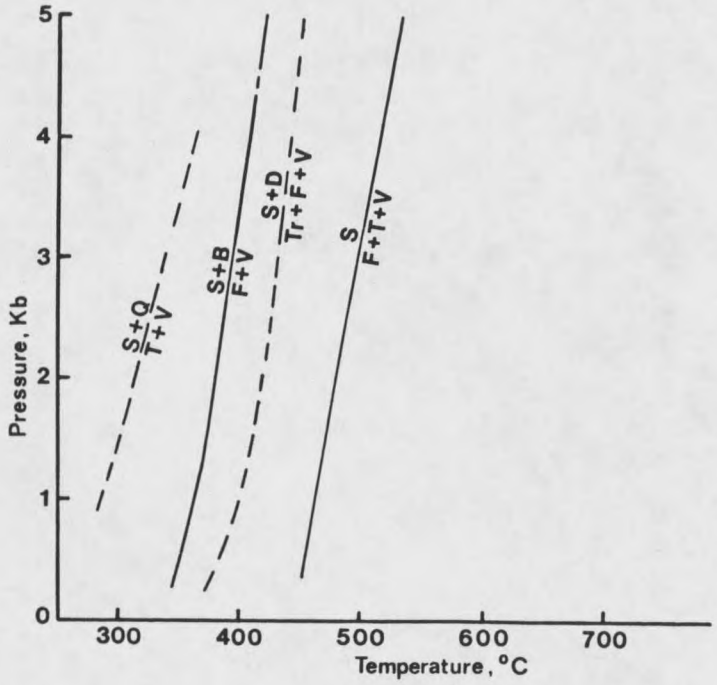

Figure 17. Temperature-Pressure diagram showing serpentine-talc relationships. S (serpentine), Q (quartz), T (talc), B (brucite), F (forsterite), Tr (tremolite), V = vapor (modified from Springer, 1974).

Several possibilities exist for heat sources which may have caused talc-forming thermal pulses. Among these are: 1) thermal resetting of K-Ar clocks, which occurred at approximately 1600 Ma.; 2) multiple generations of mafic dikes were intruded in the region between 1700 Ma. and 1100 Ma. (Wooden and others, 1968); and 3) thermal effects related to Phanerozoic deformation.

Phanerozoic timing of talc formation is unlikely, in that talc formation is not observed in favorable dolomitic host rocks of Paleozoic age in the central and northern Ruby Range, which are closely related spatially to Archean marbles with abundant talc (Tysdal, 1970; Garihan, 1973). Also, wide-spread thermal effects are not generally

associated with Phanerozoic deformation in southwestern Montana, with the exception of Mesozoic intrusives. However, such intrusives have not been recognized in the Ruby Range. These points indicate that talc formation preceded deposition of Phanerozoic sediments.

The possibility exists that resetting of K-Ar clocks and intrusion of mafic dikes are manifestations of a proposed higher heat flow in the region, associated with rifting of the Belt Basin. The theory of relatively higher heat flow during mid-to late-Proterozoic time is proposed by analogy with present-day rift environments. One example is the Great Basin of the western United States, where a relatively higher geothermal gradient exists due to extensional tectonics resulting from crustal attenuation (Lachenbruch and Sass, 1978). A similar tectonic framework existed in southwestern Montana during middle-to late-Proterozoic time, marked by development of the Belt Basin (McMannis, 1963; Schmidt and Garihan, 1986). It therefore seems reasonable to assume that extension related to rifting of the Belt Basin would have produced a relatively higher geothermal gradient in the region, thus providing a possible heat source for talc formation on a regional scale.

A Proterozoic age for talc formation is indicated from the discussion presented above. This age agrees with that proposed in previous studies (Okuma, 1971; Garihan, 1973; Berg, 1979). As noted above, several possibilities exist for a source of heat to generate growth of talc during this time period: 1) thermal resetting of K-Ar geologic clocks; 2) intrusion of multiple generations of mafic dikes in the region between 1700 Ma. and 1100 Ma.; and 3) the tectonic setting

proposed by Schimdt and Garihan (1983) for the region during middle-to late-Proterozoic time suggests a locally higher geothermal gradient due to the extensional regime associated with opening of the Belt Basin.

Summary

The metamorphic history of the study area, microscopic-scale textural relationships, and the tectonic setting of the study area are all consistent with talc formation occurring very late-to post-greenschist thermal metamorphism, dated at 1600 Ma.. The localized, podiform nature of talc bodies and the fluid flux necessary for talc formation suggest that economically viable talc bodies did not form in response to a regional thermal metamorphic event. An absolute age for talc formation in the range 1600 Ma. to 1100 Ma. is proposed.

CHAPTER 6

PHYSICAL CONDITIONS OF TALC FORMATION

Introduction

In developing a model for formation of economic-sized talc bodies the determination of temperature and pressure conditions of talc formation is critical. The talc stability field is fairly well defined in terms of temperature (T) and mole fraction CO_2 (X_{CO2}) of the fluid phase, varying with changes in pressure (Gordon and Greenwood, 1970; Skippen, 1974). In order to place constraints on possible temperatures of talc formation observed during this study, it is thus necessary to establish pressure conditions, hence the depth of burial of the marbles under examination.

Pressure of Talc Formation

The Dillon Block (Harrison, 1974), (Figure 1) has been interpreted as an exposed highland during late Proterozoic time, serving as the source area for marble, gneiss, and amphibolite clasts found within the LaHood Formation of the Belt Supergroup (McMannis, 1968; Boyce, 1975). This interpretation places the study area in a near surface environment during the time period deemed most feasible for talc formation. It is not possible however, to define an exact depth for talc formation with data currently available. A depth range of 0 km to 6 km, with a

corresponding maximum pressure (P) of 2 kbar, is consistent with a near surface interpretation, and will be used in the following discussion on temperature of talc formation.

Temperature of Talc Formation

Introduction

Limits on the temperature of formation of talc deposits can be determined by examination of the stability of talc on a temperature-X_{CO2} ($T\text{-}X_{CO2}$) diagram. The stability field of talc has been well defined by the theoretical and experimental work of several investigators who have studied the system $CaO\text{-}MgO\text{-}SiO_2\text{-}H_2O\text{-}CO_2$. Bowen (1940) noted that progressive metamorphism of dolomitic marbles involves a combination of decarbonation and dehydration reactions. Korzhinskii (1959) demonstrated that the temperature of any given reaction in this system will vary as a function of the CO_2 content of fluids present during metamorphism at constant pressure. Later investigators graphically illustrated these relationships using $T\text{-}X_{CO2}$ diagrams (Metz and Trommsdorff, 1968; Gordon and Greenwood, 1970; Skippen, 1971, 1974; Slaughter and others, 1975). An isobaric $T\text{-}X_{CO2}$ diagram outlining the talc stability field is shown in Figure 18.

It should be noted here that the salinity of fluids which affected talc formation can not be determined with the methodology used in this study. Consequently, elevation or depression of the temperature of talc formation due to the presence of a saline component in talc-forming fluids will not be addressed. The fluid phase will be assumed to have been a binary mixture of H_2O and CO_2.

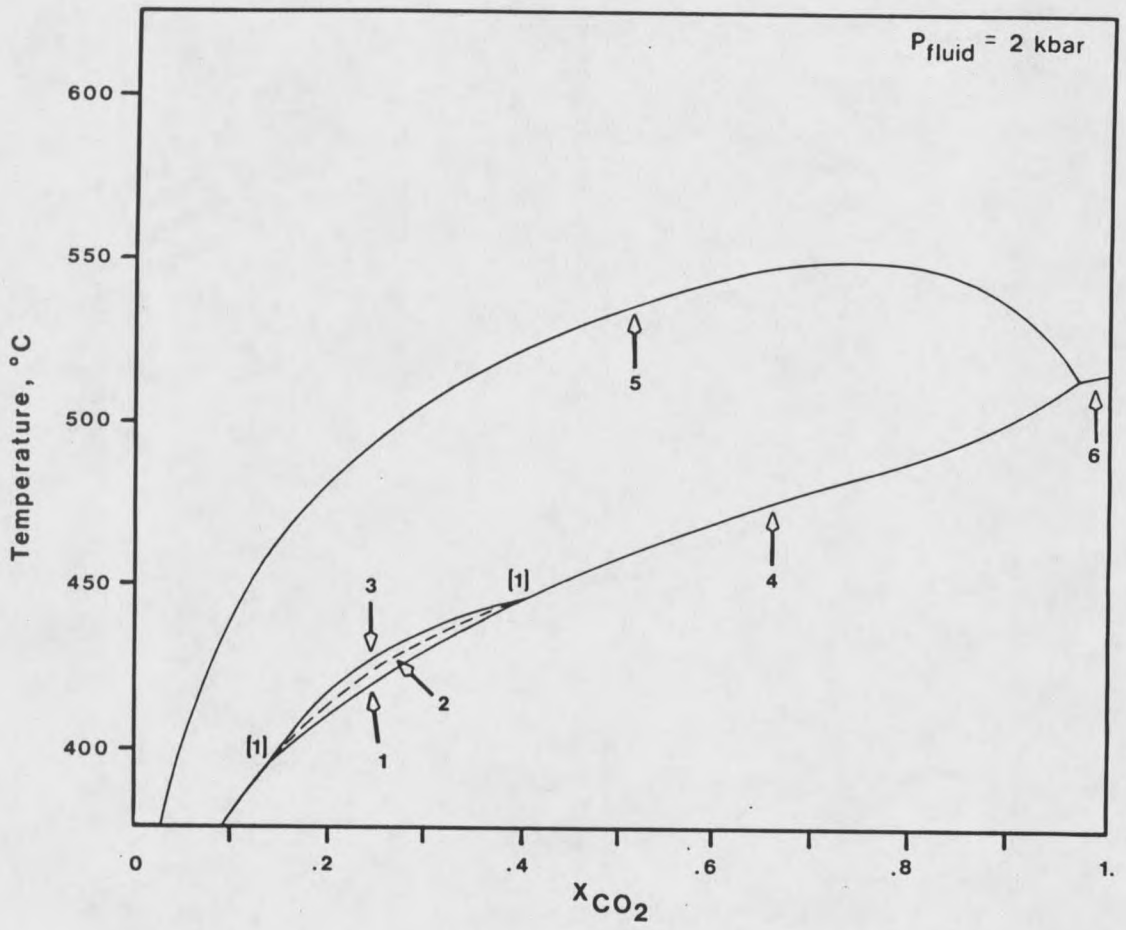

Reaction:

1) 3 Do + 4 Qtz + H_2O = 1 Tc + 3 Cc + 3 CO_2
2) 5 Tc + 6 Cc + 4 Qtz = 3 Tr + 6 CO_2 + 2 H_2O
3) 2 Tc + 3 Cc = 1 Tr + 1 Do + 1 CO_2 + H_2O
4) 8 Qtz + 5 Do + H_2O = 1 Tr + 3 Cc + 7 CO_2
5) 1 Tr + 3 Cc + 2 Qtz = 5 Di + 3 CO_2 + 1 H_2
6) 1 Do + 2 Qtz = 1 Di + 2 CO_2
7) (1) = Invariant Point 1

Figure 18. Isobaric Temperature-X_{CO2} diagram showing the stability field of talc at P_{fluid} = 2 kbar. Do (dolomite), Qtz (quartz), Tc (talc), Tr (tremolite), Cc (calcite), Di (diopside) (modified from Skippen, 1974).

Talc Stability Field

An isobaric T-X_{CO2} diagram outlining the talc stability field (TSF) for calcite-bearing marbles at a pressure of 2 kbar is shown in Figure 18. By inspection it is seen that the TSF is bounded by isobaric univariant curves 1 and 3, with limits on talc formation at P_{fluid} = 2 kbar of 400°–450° C at X_{CO2} = 0.15–0.4. Reactions 1, 2, 3 and 4 from Figure 18 are isobaric univariant reactions, and would be expected to buffer X_{CO2} during prograde metamorphism (Skippen, 1971, 1974; Greenwood, 1975; Rice, 1977a; 1977b; Ferry and Burt, 1982; Rice and Ferry, 1982; Flowers and Helgeson, 1983).

Talc-bearing marbles in the Ruby Range are dolomitic and no univariant assemblages have been documented in this study. High-variance mineral parageneses are indicated; therefore invariant point(s) 1 in Figure 18 will not exist. This allows Reaction 1 to continue to the H_2O-rich side of Figure 18, becoming asymptotic with respect to the Y axis under extremely H_2O-rich conditions.

Field and petrographic observations suggest that talc formed in an open system. The absence of isobaric univariant mineral assemblages indicates a lack of buffering capacity by dolomitic marbles, thus external control (infiltration) of the fluid phase during talc formation is indicated. These points are consistent with metasomatic introduction of SiO_2 and Mg^{++} as previously presented.

Mass balance calculations demonstrate that 15,542 moles of CO_2 are liberated during formation of talc from 1 m^3 of dolomitic marble, with a minimum fluid flux of 7×10^5 liters (39×10^6 moles) H_2O. This results in $X_{CO2} = 3.98 \times 10^{-4}$ ($X_{CO2} = CO_2/H_2O + CO_2$), with CO_2 being

extremely diluted by infiltrating solutions. This dilution would allow talc formation at extremely low temperatures due to the asymptotic nature of Reaction 1 with respect to the H_2O-rich side of Figure 18, as described above.

It should be noted that talc also occurs at higher temperatures than those described here, either due to the presence of impurities such as Fe, or as a metastable phase (Figure 17). However, phase equilibria and mineral relationships noted during this study allow high-temperature talc formation to be discounted as an important talc-forming mechanism. Since talc is metastable in high-temperature environments, such occurrences are not considered as viable mechanisms for talc formation on an economic scale. Also, high-temperature mineral assemblages stably coexisting with talc were nowhere observed during this study, while it has been noted that recrystallization of low temperature phases such as serpentine to form talc is common (Tables 1 and 2). For these reasons consideration of possible temperature conditions prevailing during talc formation are limited to a maximum of 450° C, and possibly considerably lower.

Summary

From the above discussion, talc formation as observed in the Ruby Range occurred below a maximum temperature of 450° C at $P_{fluid} = 2$ kbar. External control of the fluid phase is indicated, and the possibility exists that infiltration of an H_2O-rich fluid allowed talc formation to occur at much lower temperatures.

CHAPTER 7

CONCLUSIONS

Timing of Talc Formation

Field and petrographic relationships, and phase equilibria, combine to place talc formation within a relative time framework. Temperature constraints on phase equilibria in the $CaO-MgO-SiO_2-H_2O-CO_2$ system indicate that talc formation must have occurred after an amphibolite-to lower-granulite-grade dynamothermal metamorphic event, dated at 2750 Ma. (James and Hedge, 1980). Further, petrographic observations indicate that talc formation was the last major event in the paragenetic sequence since talc replaces dolomite and nearly all greenschist-grade silicate minerals present. Formation of greenschist-grade minerals occurred during Proterozoic retrograde thermal metamorphism dated at 1600 Ma. (Giletti, 1966). The maximum age indicated for talc formation based on the metamorphic history and the paragenetic sequence is thus very late-to post-greenschist-grade thermal metamorphism, dated at approximately 1600 Ma.

Talc is not found within favorable dolomitic horizons in Paleozoic rocks which are closely related spatially to talc-bearing Archean marbles. This strongly suggests that talc formation was a pre-Paleozoic event. Timing of talc formation is thus constrained to the Proterozoic Eon, and further, late-to post-greenschist metamorphism, with a probable maximum age of talc formation of 1600 Ma.

The thermal history interpreted from the paragenetic sequence suggests that talc may have formed as a natural result of retrograde metamorphism, as described in previous studies (Okuma, 1971; Garihan, 1973; Berg, 1979). However, ubiquitous replacement of serpentine by talc requires that a late, or secondary, thermal pulse accompanied talc formation. Also, mass balance calculations indicate that significant volumes of water must have moved through each localized talc-forming system. Such features are not normally associated with regional metamorphic cycles. Therefore, a late-or post-greenschist age for talc formation is favored.

Physical Conditions of Talc Formation

The study area has been described as a positive tectonic element during middle-to late-Proterozoic time, placing marbles of the area in a near surface environment during the time period proposed for talc formation.

Phase equilibria of the system $CaO-MgO-SiO_2-H_2O-CO_2$ indicate a relatively narrow stability field for talc formation at low pressures, with the talc stability field becoming asymptotic with respect to the H_2O side of the diagram. The isobaric $T-X_{CO2}$ diagram in Figure 18 shows that the maximum temperature for talc formation at an assumed P_{fluid} of 2 kbar is 450° C at $X_{CO2} = 0.4$.

X_{CO2} probably approached 0.0 during talc formation due to the large quantities of H_2O necessary to transport all SiO_2 for talc formation, and the relatively small amounts of CO_2 produced by talc

formation. This would allow talc formation at much lower temperatures than that stated above.

Mechanism of Talc Formation

All aspects of this study aid in the development of the proposed model for talc formation. The salient features used to develop this model are summarized here.

1) Field and petrographic observations indicate that: 1) talc formation was the last major event in the paragenetic sequence; 2) calcite, which formed as a by-product of the main talc-forming reaction, has been removed from the system; 3) talc formation was a localized process, with strong structural controls indicated; and 4) constant volume was maintained during talc formation.

2) Mass balance calculations and whole rock geochemistry indicate that large quantities of SiO_2, Mg^{++}, and H_2O were added to the system. Two stages of infiltration are indicated, possibly overlapping in time. The first stage is marked by dolomitization with concomitant increases in MgO/SiO_2 ratios, followed by second stage silicification, resulting in talc formation.

3) Formation of talc is proposed to have been in a near surface environment ($P_{fluid} < 2$ kbar), based on interpretations of the tectonic history of the study area.

4) Maximum temperature of talc formation at the depth indicated above is 450° C. The presence of an H_2O-rich fluid phase would permit talc formation at much lower temperatures.

These data are all consistent with talc formation resulting from hydrothermal activity in a hot springs environment. Fluids venting to the land surface in such a system may have provided the mechanism by which calcite and CO_2 were removed from the system.

The heat source necessary to drive the talc-forming reaction(s) may have been provided by the naturally high geothermal gradient which should have accompanied the extensional environment of the Proterozoic Belt Basin, or by igneous activity related to Proterozoic-aged mafic dike swarms. Due to the scattered and discontinuous nature of talc occurrences, and the apparent lack of mafic dikes spatially related to talc prospects examined, the regionally high geothermal gradient would seem to be the most plausible mechanism for heating of fluids on a localized scale without associated igneous activity. By analogy, heating of meteoric waters by circulation at depth along fault zones, without related igneous activity, is a relatively common occurrence in southwestern Montana at the present time (Sondregger and others, 1982).

Significance of Study

The model presented here for talc formation in Archean dolomitic marbles differs from that proposed by many previous studies (Okuma, 1971; Garihan, 1973; Olson, 1976; Berg, 1979; Karasevich and others, 1981; Piniazkiewicz, 1984). This model may be applicable to other known talc occurrences in similar host rocks in southwestern Montana,

the major difference in each case being the scale of the hot springs system necessary to accomodate the observed volume of talc formation.

It should be apparent that much work still remains before the physical and chemical controls on formation of such talc deposits are well understood. Hopefully this study will illuminate several possible lines of further research which may contribute further information to what is currently known about one of the most crucial aspects of talc formation in southwestern Montana, that is, the fluids which caused formation of talc within dolomitic marbles of Archean age.

REFERENCES CITED

REFERENCES CITED

Berg, R.B., 1979, Talc and chlorite deposits in Montana: Montana Bureau of Mines and Geology Memoir 45, 66 p.

Bielak, J., 1978, The origin of Cherry Creek amphibolites from the Winnipeg Creek area of the Ruby Range, Southwestern Montana: M.S. Thesis, University of Montana, 46 p.

Bowen, N.L., 1940, Progressive metamorphism of siliceous limestone and dolomite: Journal of Geology, v. 48, p. 225-274.

Bergantino, R.N., and Clark, M.C., 1985, Structure contour map on the top of Precambrian crystalline rocks, Montana: Montana Bureau of Mines and Geology Open File Report 158.

Boyce, Robert L., 1975, Depositional systems in the LaHood Formation, Belt Supergroup, Precambrian, Southwestern Montana: Ph.D. dissertation, The University of Texas at Austin, 247 p.

Dahl, P., 1979, Comparative geothermometry based on major element and oxygen isotope distributions in Precambrian metamorphic rocks from southwestern Montana: American Mineralogist, v. 64, p. 1280-1293.

Desmarais, N.R., 1981, Metamorphosed Precambrian ultramafic rocks in the Ruby Range, Montana: Precambrian Research, v. 16, p. 67-101.

Ellis, A.J., and Mahon, W.J., 1977, Chemistry and geothermal systems: Academic Press, New York, 392 p.

Ferry, J.M., and Burt, J.M., 1982, Characterization of metamorphic fluid composition through mineral equilibria, in Ferry, J.M., ed., Characterization of metamorphism through mineral equilibria: Reviews in Mineralogy (v. 10), Mineralogic Society of America, p. 207-262.

Flowers, G.C., and Helgeson, H.C., 1983, Equilibrium and mass transfer during progressive metamorphism of siliceous dolomites: American Journal of Science, v. 283, p. 230-286.

Garihan, 1973, Geology and talc deposits of the central Ruby Range, Madison County, Montana: unpublished Ph.D. dissertation, Pennsylvania State University, 209 p.

Garihan, J.M., and Okuma, A.F., 1974, Field evidence suggesting a non-igneous origin for the Dillon quartzofeldspathic gneiss, Ruby Range, southwestern Montana (abs): Geologic Society of America Abstracts with Programs, v. 6, no. 6, p. 510.

Gordon, T.M., and Greenwood, H.J., 1970, The reaction: Dolomite + Quartz + Water = Talc + Calcite + Carbon Dioxide: American Journal of Science, v. 268, p. 225-242.

Greenwood, H.J., 1975, Buffering of pore fluids by metamorphic reactions: American Journal of Science, v. 275, p. 573-593.

Harrison, J.E., Griggs, A.B., and Wells, J.D., 1974, Tectonic features of the Precambrian Belt Basin and their influence on post-Belt structures: U. S. Geologic Survey Professional Paper 866, 15 p.

Heinrich, W., and Rabbitt, J.C., 1960, Pre-Beltian geology of the Cherry Creek and Ruby Mountains areas, southwestern Montana: Montana Bureau of Mines and Geology Memoir 38, 40 p.

James, H.L., and Hedge, C.E., 1980, Age of the basement rocks of southwest Montana: Geological Society of America Bulletin, v. 91, p. 11-15.

Klepper, M. R., 1950, A geologic reconnaissance of parts of Beaverhead and Madison Counties, Montana: U. S. Geological Survey Bulletin 969-C, p. 55-85.

Korzhinskii, D.S., 1959, Physicochemical basis of the analysis of the paragenesis of minerals, Consultants Bureau Incorporated, New York, 142 p.

Karasevich, L.P., Garihan, J.M., Dahl, P.S., and Okuma, A.F., 1981, Summary of Precambrian metamorphic and structural history, Ruby Range, southwest Montana: Montana Geologic Society 1981 Field Conference, p. 225-237.

Lachenbruch, A.H., and Sass, J.H., 1978, Models of an extending lithosphere and heat flow in the Basin and Range province, in Smith, R.B., and Eaton, G.P., eds., Cenozoic tectonics and regional geophysics of the western Cordillera: Geological Society of America Memoir 152, p. 209-250.

Levinson, A.A., 1949, Petrography of pre-Beltian Cherry Creek Marbles, southwestern Montana: unpublished M.S. thesis, University of Michigan, 46 p.

McMannis, W.J., 1963, LaHood Formation - A coarse facies of the Belt Series in southwestern Montana: Geological Society of America Bulletin, v. 74, p. 407-436.

Metz, P., and Trommsdorff, V., 1968, On phase equilibria in metamorphosed siliceous dolomites: Contributions to Mineralogy and Petrology, v. 18, p. 305-309.

Morey, G.W., and Hesselgesser, J.M., 1951, The solubility of some minerals in superheated steam at high pressures: Economic Geology, v. 46, p. 821-835.

Okuma, A. F., 1971, Structure of the southwestern Ruby Range near Dillon Montana: unpublished Ph.D. dissertation, Pennsylvania State University, 122 p.

Olson, R. H., 1976, The geology of Montana talc deposits, in Eleventh Industrial Minerals Forum: Montana Bureau of Mines and Geology Special Publication 74, p. 99-143.

Peale, A.C., 1896, Description of the Three Forks Sheet, Montana: U.S. Geologic Survey, Geologic Atlas, Three Forks Folio, no. 24, 5 p.

Perry, E.S., 1948, Talc, graphite, vermiculite, and asbestos in Montana: Montana Bureau of Mines and Geology Memoir 27, 44 p.

Piniazkiewicz, R.J., 1984, Geology and exploration techniques for Pre-Beltian talc on the Malesich Ranch, Ruby Range, Madison County, Montana: M.S. Thesis, University of Arizona, 101 p.

Rice, J.M., 1977a, Progressive metamorphism of impure dolomitic limestone in the Marysville aureole, Montana: American Journal of Science, v. 277, p. 1-24.

_____. 1977b, Contact metamorphism of impure dolomitic in the Boulder aureole, Montana: Contributions to Mineralogy and Petrology, v. 59, p. 237-259.

Rice, J.M., and Ferry, J.M., 1982, Buffering, infiltration, and the control of intensive variables during metamorphism, in Ferry, J.M., ed., Characterization of metamorphism through mineral equilibria: Reviews in Mineralogy (v. 10), Mineralogic Society of America, p. 263-326.

Robie R.A., Hemingway, B. S., and Fisher, J.R., 1979, Thermodynamic properties of minerals and related substances at 298.15 K and 1 bar pressure and at higher temperatures: U. S. Geological Survey Bulletin 1452, 456 p.

Schmidt, C.J., and Garihan, J.M., 1983, Laramide tectonic development of the Rocky Mountain Foreland of southwestern Montana, in Lowell, J.D., ed., Rocky Mountain Foreland Basins and Uplifts: Rocky Mountain Association of Geologists, p. 271-294.

Schmidt, C. J., and Garihan, J.M., 1986, Middle Proterozoic and Laramide tectonic activity along the southern margin of the Belt Basin: Montana Bureau of Mines and Geology Special Publication 94, p. 217-235.

Skippen, G., 1974, An experimental model for low pressure metamorphism of siliceous dolomitic marble: American Journal of Science, v. 274, p. 487-509.

Slaughter, J., Kerrick, D.M., and V.J. Wall, 1975, Experimental study of equilibria in the system $CaO-MgO-SiO_2-H_2O-CO_2$: American Journal of Science, v. 275, p. 143-162.

Smith, K., 1977, Petrology and origin of Precambrian metamorphic rocks in the eastern Ruby Mountains, Southwestern Montana: M.S. Thesis, University of Montana, 84 p.

Sonderegger, J.L., Schofield, J.D., Berg, R.B., and Mannick, M.L., 1982, The upper Centennial Valley, Beaverhead and Madison Counties, Montana - An investigation of resources utilizing geological, geophysical, hydrochemical and geothermal methods: Montana Bureau of Mines and Geology Memoir 50, 53 p.

Springer, R.K., 1974, Metamorphosed ultramafic rocks in California: Journal of Petrology, v. 15, p. 160-195.

Tysdal, R.G., 1976, Geologic map of northern part of Ruby Range, Madison County, Montana: U. S. Geologic Survey Miscellaneous Investigations Series, Map I-951.

Walton, K., 1981, A study of the Treasure Chest talc mine and other talc deposits in southwestern Montana: Senior Thesis, Smith College, Northhampton, Massachusetts, 30 p.

Weill, D.F., and Fyfe, W.S., 1964, The solubility of quartz in H_2O in the range 1000-4000 bars and 400-550° C: Geochimica et Cosmochimica Acta, v. 28, p. 1243-1255.

Whitehead, M., 1979, Geology and talc occurrences of the Benson Ranch Beaverhead County, Montana: M.S. Thesis, Montana College of Mineral Science and Technology, 53 p.

Winston, D., 1986, Middle Proterozoic tectonics of the Belt Basin, western Montana and northern Idaho: Montana Bureau of Mines and Geology Special Publication 94, p.245-257.

Wood, J.A., 1958, The solubility of quartz in water at high temperatures and pressures: American Journal of Science, v. 256, p. 40-47.

Wooden, J.L., Vitalianio, C.J., Koehler, S.W., and Ragland, P.C., 1978, The late Precambrian mafic dikes of the southern Tobacco Root Mountains, Montana: geochemistry, Rb-Sr geochronology and relationship to Belt tectonics: Canadian Journal of Earth Sciences, v. 15, no. 4, p. 467-479.

APPENDIX

WHOLE ROCK GEOCHEMICAL ANALYSES

Table 7. Whole rock geochemical analyses of high-grade marble. Samples were analysed using X-Ray fluorescence, by XRAL Inc.. Area designators are: AB (Bosal Prospect), AR (Ruby View Prospect), AT (T.P. Prospect), AS (Spring Creek Prospect), AP (Pope Prospect), ASW (Sweetwater Mine).

	AB-71	AP-36	AS-68	ASW-18	AT-28	AT-31
SiO_2	13.30	7.88	1.03	3.78	3.48	5.81
Al_2O_3	0.32	0.18	0.13	0.14	0.52	0.19
CaO	34.20	50.50	30.00	29.00	29.40	34.00
MgO	16.60	2.61	21.20	21.30	20.40	17.30
Na_2O	<0.01	<0.01	<0.01	<0.01	<0.01	<0.01
K_2O	0.13	0.06	0.03	0.03	0.04	0.04
Fe_2O_3	0.63	0.44	1.50	0.86	1.11	0.70
MnO	0.74	0.63	0.84	0.75	1.00	0.73
TiO_2	0.03	<0.01	0.02	0.02	0.04	0.01
P_2O_5	0.02	0.02	0.04	0.02	0.02	0.02
Cr_2O_3	<0.01	<0.01	<0.01	<0.01	<0.01	<0.01
LOI	34.00	37.50	45.20	44.60	44.50	41.70
Sum	98.97	99.82	99.99	100.50	100.51	100.50

	AR-49
SiO_2	14.20
Al_2O_3	<0.01
CaO	36.50
MgO	14.10
Na_2O	<0.01
K_2O	0.03
Fe_2O_3	0.95
MnO	0.77
TiO_2	<0.01
P_2O_5	0.02
Cr_2O_3	<0.01
LOI	33.40
Sum	99.97

Table 8. Whole rock geochemical analyses of talc-bearing marble. Samples were analysed using X-Ray fluorescence, by XRAL Inc.. Area designators are: AB (Bosal Prospect), AR (Ruby View Prospect), AT (T.P. Prospect), AS (Spring Creek Prospect), AP (Pope Prospect), ASW (Sweetwater Mine).

	AB-65	AB-70	AP-37	AS-69	AS-70	ASW-19
SiO_2	14.00	17.70	6.64	8.33	4.88	4.97
Al_2O_3	0.25	0.41	0.52	0.22	0.48	0.15
CaO	23.40	24.10	27.40	26.60	28.00	0.55
MgO	24.00	21.40	22.90	23.00	22.30	49.00
Na_2O	<0.01	<0.01	<0.01	<0.01	<0.01	<0.01
K_2O	0.04	0.04	0.03	0.03	0.04	0.03
Fe_2O_3	1.20	1.40	0.92	1.44	1.08	1.96
MnO	0.10	0.28	0.27	0.45	0.56	0.22
TiO_2	0.03	0.02	0.04	0.01	0.04	0.03
P_2O_5	0.02	0.02	0.02	0.02	0.03	0.03
Cr_2O_3	<0.01	<0.01	<0.01	<0.01	<0.01	<0.01
LOI	37.40	35.00	41.80	40.50	42.80	43.30
Sum	100.44	100.37	100.31	100.24	100.54	100.60

	AT-23	AT-24	AT-25	AT-26	AR-30	AR-33
SiO_2	5.15	2.63	5.35	8.13	3.04	14.50
Al_2O_3	0.49	0.14	0.42	0.24	0.04	<0.01
CaO	27.40	29.50	27.60	26.30	25.50	23.80
MgO	21.20	21.40	22.00	21.30	25.40	24.00
Na_2O	<0.01	<0.01	<0.01	<0.01	<0.01	<0.01
K_2O	0.04	0.03	0.04	0.04	0.03	0.04
Fe_2O_3	3.18	1.64	1.51	3.20	0.95	1.00
MnO	0.88	0.91	0.88	0.84	0.12	0.60
TiO_2	0.03	0.01	0.03	0.02	0.02	0.01
P_2O_5	0.02	0.02	0.02	0.02	0.02	0.02
Cr_2O_3	<0.01	<0.01	<0.01	<0.01	<0.01	<0.01
LOI	42.20	44.20	42.40	40.20	45.20	36.50
Sum	100.59	100.48	100.25	100.29	100.32	100.47

Table 8--Continued

	AR-34	AR-47
SiO_2	22.30	11.60
Al_2O_3	0.01	0.62
CaO	19.30	18.70
MgO	25.50	28.30
Na_2O	<0.01	<0.01
K_2O	0.04	0.04
Fe_2O_3	1.54	1.46
MnO	0.17	0.15
TiO_2	0.02	0.05
P_2O_5	0.02	0.02
Cr_2O_3	<0.01	<0.01
LOI	31.50	39.50
Sum	100.4	100.44

Table 9. Whole rock geochemical analyses of talc. Samples were analysed using X-Ray fluorescence, by XRAL Inc.. Area designators are: AB (Bosal Prospect), AR (Ruby View Prospect), AT (T.P. Prospect), AS (Spring Creek Prospect), AP (Pope Prospect), ASW (Sweetwater Mine).

	AB-67	AP-39	AS-71	ASW-21	AT-21	AR-35
SiO_2	60.00	59.00	58.50	60.10	59.90	60.50
Al_2O_3	0.46	1.20	1.02	0.55	0.09	0.03
CaO	0.15	0.17	0.08	0.30	0.01	0.13
MgO	32.20	32.10	31.80	32.50	27.80	31.70
Na_2O	<0.01	<0.01	<0.01	0.05	<0.01	<0.01
K_2O	0.03	0.03	0.04	0.01	0.03	0.04
Fe_2O_3	0.44	0.78	0.83	0.27	6.80	1.02
MnO	0.01	0.01	0.01	0.01	0.01	0.05
TiO_2	0.04	0.07	0.07	0.04	0.02	0.02
P_2O_5	0.02	0.09	0.01	0.17	0.02	0.02
Cr_2O_3	<0.01	<0.01	<0.01	<0.01	<0.01	<0.01
LOI	6.08	6.31	6.08	5.70	4.93	5.47
Sum	99.43	99.76	98.44	99.71	99.61	98.98

Table 10. Whole rock geochemical analyses of gneisses. Samples were analysed using X-Ray fluorescence, by XRAL Inc.. Area designators are: AB (Bosal Prospect), ASW (Sweetwater Mine).

	ASW-15	ASW-16	ASW-17	AB-62	AB-64
SiO_2	71.40	33.00	74.10	54.20	66.50
Al_2O_3	13.60	18.10	14.40	14.50	13.70
CaO	0.38	0.24	0.53	7.35	0.28
MgO	6.13	35.00	0.13	7.16	8.20
Na_2O	<0.01	<0.01	3.75	2.08	<0.01
K_2O	3.14	0.05	5.00	0.84	3.05
Fe_2O_3	0.33	0.71	1.05	11.10	2.70
MnO	0.02	0.02	0.02	0.14	0.02
TiO_2	0.03	0.03	0.05	0.74	0.63
P_2O_5	0.01	0.02	0.10	0.09	0.19
Cr_2O_3	0.01	<0.01	0.01	0.03	0.01
LOI	4.16	13.20	0.39	2.00	5.00
Sum	99.30	100.37	99.53	100.23	100.28

PLATE I

BOSAL PROSPECT

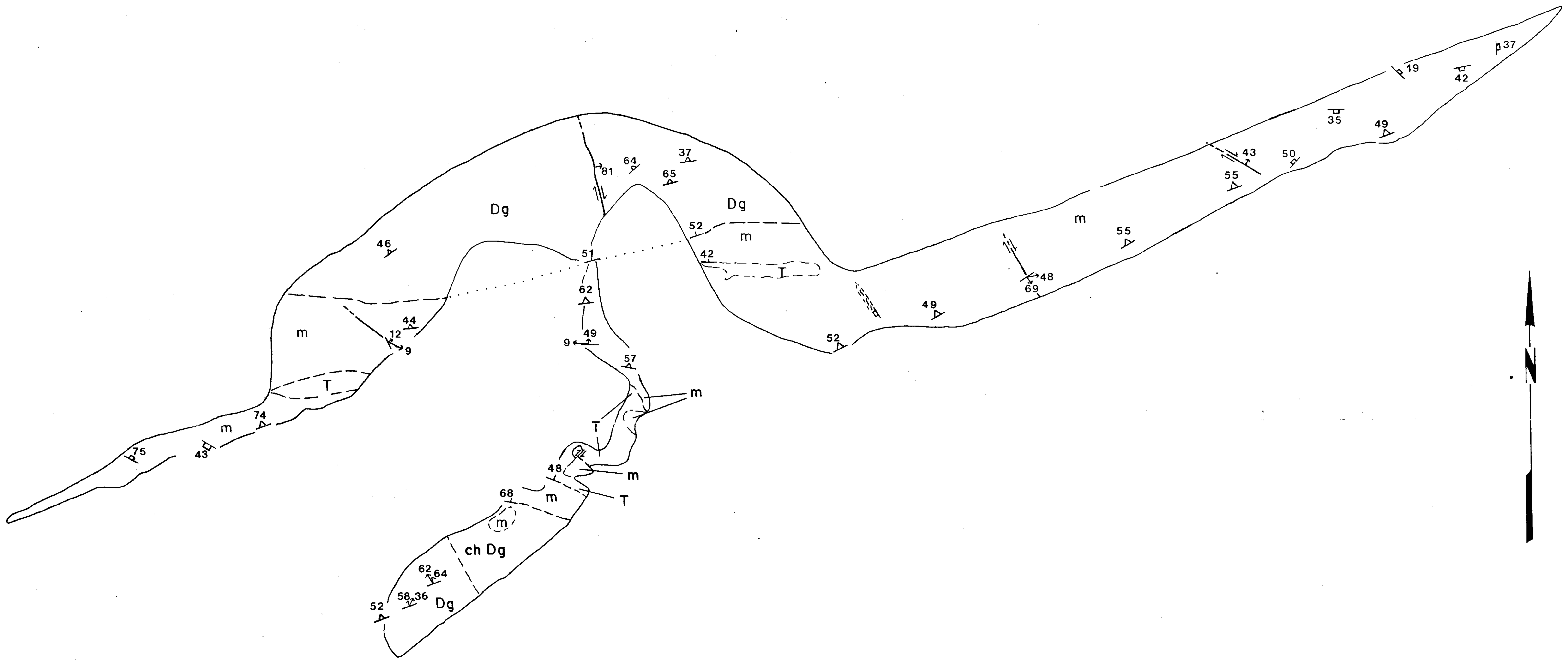

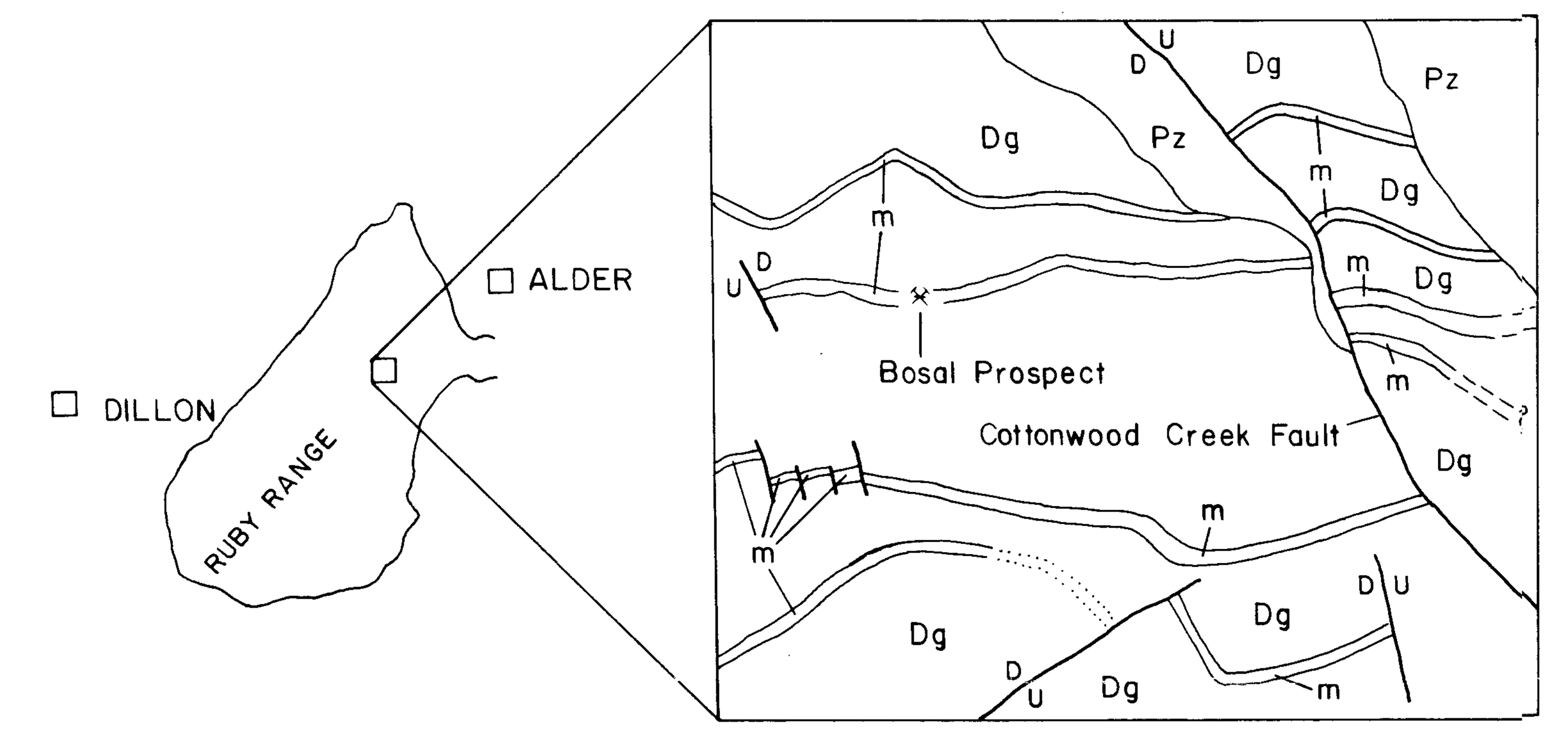

EXPLANATION

- Pz — Paleozoic Undivided
- Dg — Dillon Gneiss
- chDg — Chloritized Gneiss
- m — Marble
- T — Talc
- Fault showing dip and trend plunge of slickenside striae
- Strike and dip of joint
- Strike and dip of foliation
- Strike and dip of lithologic contact

SCALE: 1" = 10'

0 10' 20'

PLATE 2

RUBY VIEW PROSPECT

EXPLANATION

- Pz — Paleozoic Undivided
- Dg — Dillon Gneiss
- m — Marble
- T — Talc

- 9 / 7 — Fault showing dip, and trend and plunge of slickenside striae
- 55 — Strike and dip of joint
- 2 — Strike and dip of foliation
- 14 — Strike and dip of lithologic contact
- 11 — Trend and plunge of synform axis
- 10 — Trend and plunge of antiform axis

0 5' 10'

Scale: 1" = 5'

N

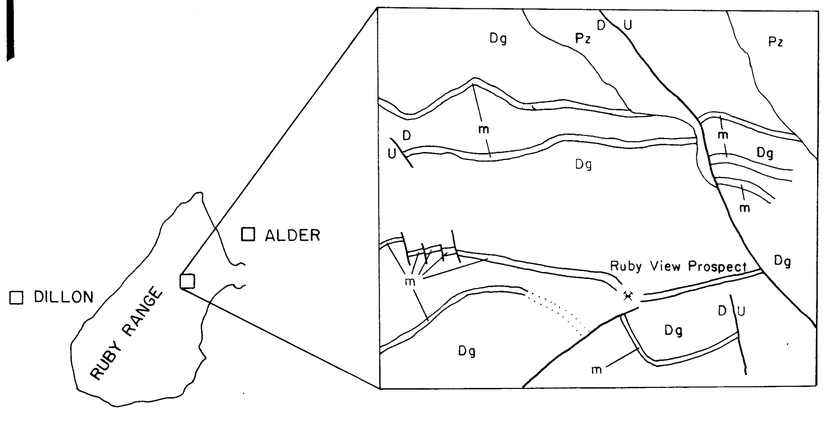

PLATE 3

T.P. PROSPECT

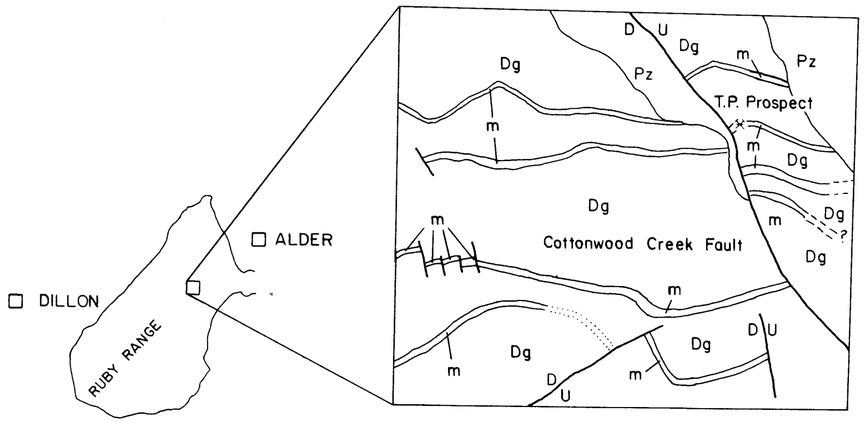

EXPLANATION

- Pz — Paleozoic Undivided
- Dg — Dillon Gneiss
- m — Marble
- T — Talc

0 10' 20'

SCALE: 1" = 10'

- 8/7 — Fault showing dip, and trend and plunge of slickenside striae
- 23 — Strike and dip of joint
- 56 — Strike and dip of foliation
- 75 — Strike and dip of lithologic contact
- Shear Zone

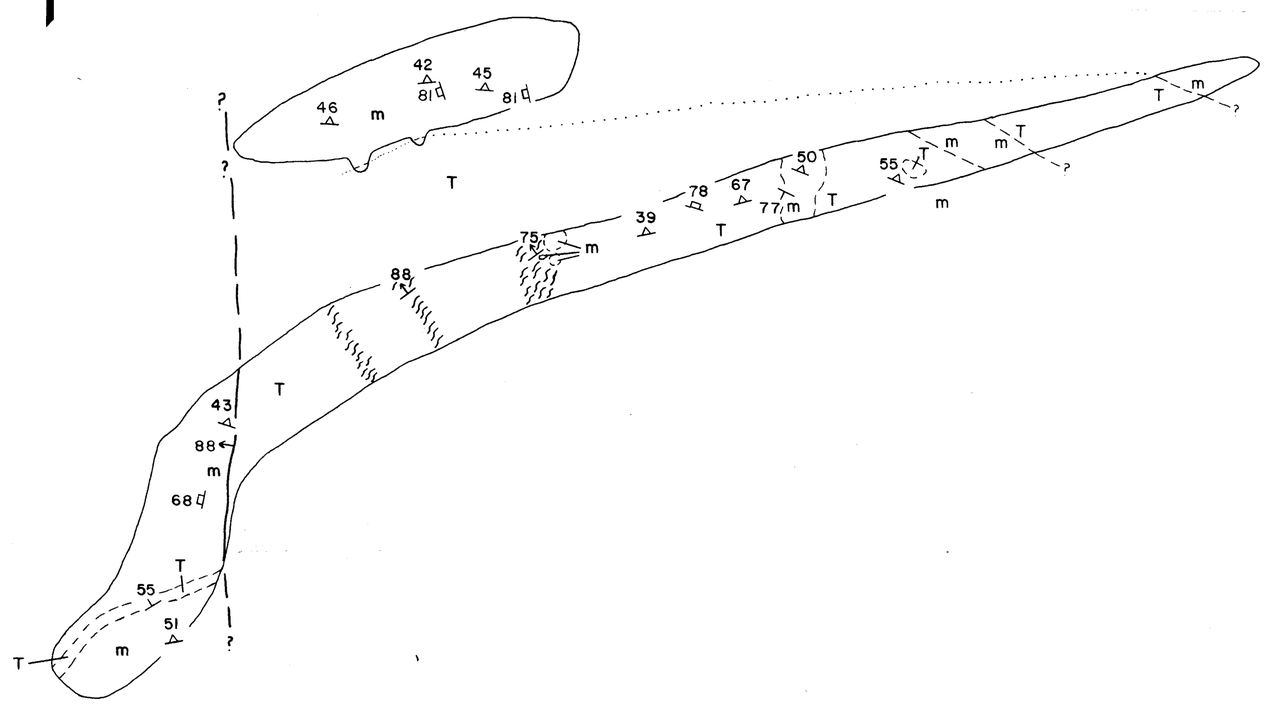

PLATE 4

SPRING CREEK PROSPECT

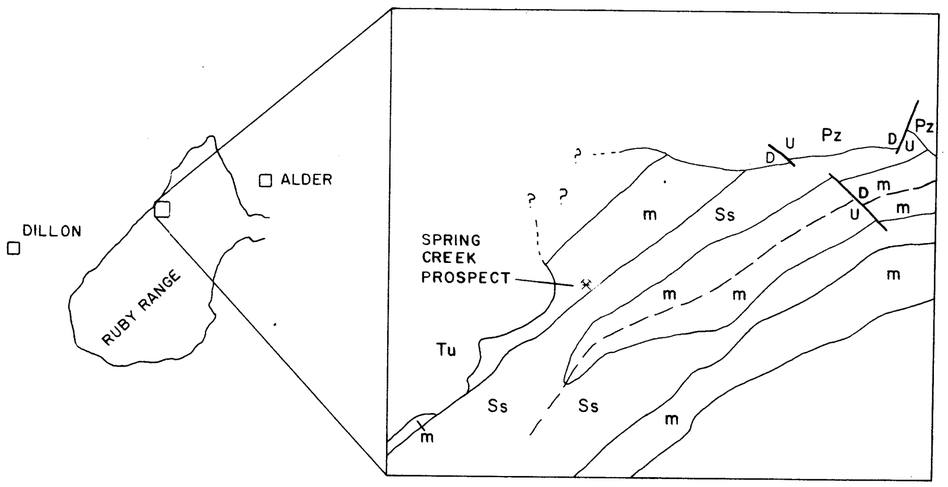

EXPLANATION

- Tu — Tertiary Undivided
- Pz — Paleozoic Undivided
- Ss — Sillimanite Schist
- m — Marble
- T — Talc

- 75 / 15 — Fault showing dip, and trend and plunge of slickenside striae
- Strike and dip of joint
- 53 — Strike and dip of foliation
- 56 — Strike and dip of lithologic contact

Scale: 1" = 10'

0 10' 20'

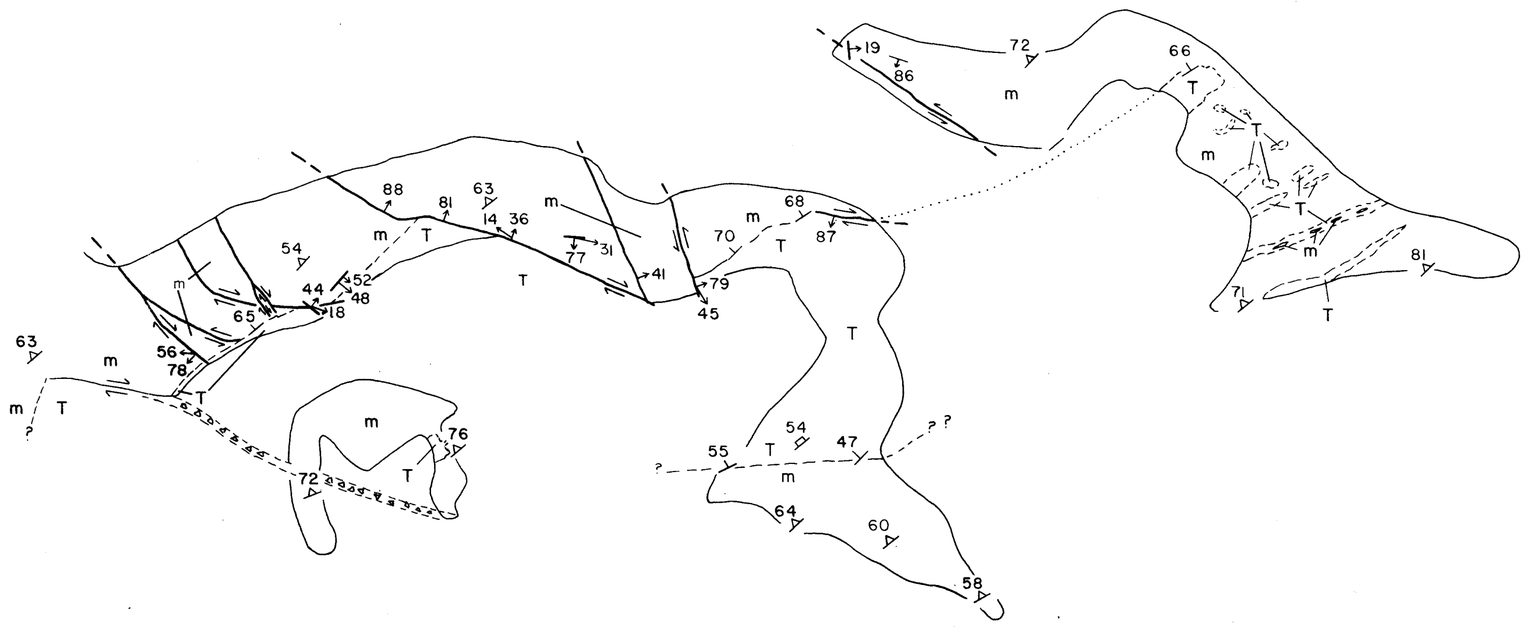

PLATE 5

POPE PROSPECT

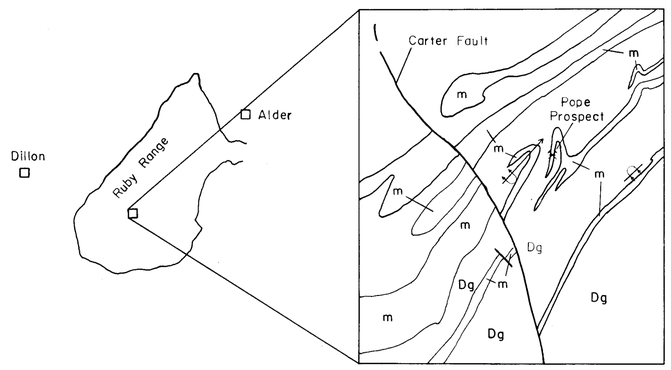

EXPLANATION

- T — Talc
- m — Marble
- s — Schist
- Dg — Dillon Gneiss

Scale: 1" = 5'

0 5' 10'

- 55 / 34 — Fault showing dip, and trend and plunge of slickenside striae
- 83 — Strike and dip of joint
- 69 — Strike and Dip of foliation
- 74 — Strike and dip of lithologic contact
- Fault zone

PLATE 6
SWEETWATER MINE

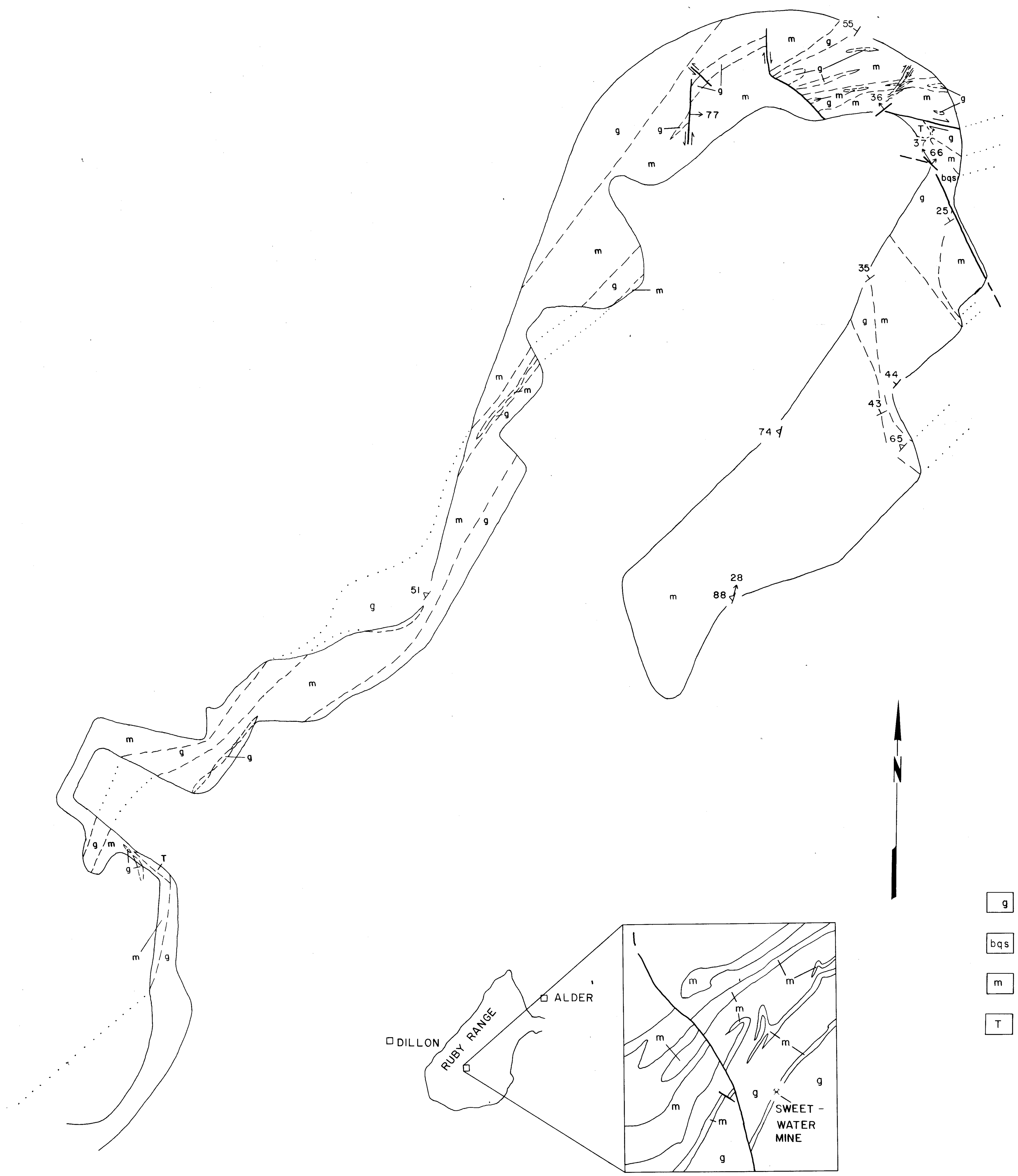

EXPLANATION

g — Gneiss

bqs — Biotite-quartz schist

m — Marble

T — Talc

23, 6 — Fault showing dip, and trend and plunge of slickenside striae

61 — Strike and dip of lithologic contact

4, 12 — Strike and dip of foliation, with lineation

Scale: 1" = 10'

0 10' 20'